

Published in final edited form as:

*J Am Chem Soc.* 2005 December 21; 127(50): 17686–17696. doi:10.1021/ja053897e.

## Spectroscopic Characterization of Interstrand Carbinolamine Crosslinks Formed in the 5'-CpG-3' Sequence by the Acrolein-Derived $\gamma$ -OH-1,N<sup>2</sup>-Propano-2'-deoxyguanosine DNA Adduct

 Young-Jin Cho, Hye-Young Kim, Hai Huang, Alvira Slutsky<sup>‡</sup>, Irina G. Minko<sup>‡</sup>, Hao Wang, Lubomir V. Nechev<sup>¶</sup>, Ivan D. Kozekov, Albena Kozekova, Pamela Tamura, Jaison Jacob<sup>§</sup>, Markus Voehler, Thomas M. Harris, R. Stephen Lloyd<sup>‡</sup>, Carmelo J. Rizzo, and Michael P. Stone

Contribution from the Department of Chemistry, Center in Molecular Toxicology, Vanderbilt-Ingram Cancer Center, Vanderbilt University, Nashville, Tennessee 37235

### Abstract

The interstrand N<sup>2</sup>,N<sup>2</sup>-dG DNA crosslinking chemistry of the acrolein-derived  $\gamma$ -OH-1,N<sup>2</sup>-propanodeoxyguanosine ( $\gamma$ -OH-PdG) adduct in the 5'-CpG-3' sequence was monitored within a dodecamer duplex by NMR spectroscopy, *in situ*, using a series of site-specific <sup>13</sup>C- and <sup>15</sup>N-edited experiments. At equilibrium 40% of the DNA was crosslinked, with the carbinolamine form of the crosslink predominating. The crosslink existed in equilibrium with the non-crosslinked N<sup>2</sup>-(3-oxopropyl)-dG aldehyde and its geminal diol hydrate. The ratio of aldehyde:diol increased at higher temperatures. The 1,N<sup>2</sup>-dG cyclic adduct was not detected. Molecular modeling suggested that the carbinolamine linkage should be capable of maintaining Watson-Crick hydrogen bonding at both of the tandem C•G base pairs. In contrast, dehydration of the carbinolamine crosslink to an imine (Schiff base) crosslink, or cyclization of the latter to form a pyrimidopurinone crosslink, was predicted to require disruption of Watson-Crick hydrogen bonding at one or both of the tandem crosslinked C•G base pairs. When the  $\gamma$ -OH-PdG adduct contained within the 5'-CpG-3' sequence was instead annealed into duplex DNA opposite T, a mixture of the 1,N<sup>2</sup>-dG cyclic adduct, the aldehyde, and the diol, but no crosslink, was observed. With this mismatched duplex, reaction with the tetrapeptide KWKK formed DNA-peptide crosslinks efficiently. When annealed opposite dA,  $\gamma$ -OH-PdG remained as the 1,N<sup>2</sup>-dG cyclic adduct although transient epimerization was detected by trapping with the peptide KWKK. The results provide a rationale for the stability of interstrand crosslinks formed by acrolein and perhaps other  $\alpha,\beta$ -unsaturated aldehydes. These sequence-specific carbinolamine crosslinks are anticipated to interfere with DNA replication and contribute to acrolein-mediated genotoxicity.

### Introduction

Acrolein **1**, a mutagen and carcinogen,<sup>1</sup> is mutagenic in bacterial,<sup>2</sup> mammalian,<sup>3</sup> and human<sup>4,5</sup> cells, and carcinogenic in rats.<sup>6</sup> It exhibits an array of chemistry in DNA, which includes the formation of cyclic hydroxylated 1,N<sup>2</sup>-propanodeoxyguanosine (OH-PdG) adducts,<sup>1,7–9</sup> and DNA interchain crosslinks<sup>10–12</sup> (Scheme 1). DNA-peptide<sup>13</sup> and DNA-

<sup>‡</sup>Center for Research on Environmental and Occupational Toxicology, Oregon Health and Science University, 3181 SW Sam Jackson Park Road, L606, Portland, OR 97239-3098

<sup>¶</sup>Current Address for Lubomir V. Nechev: Alnylam Pharmaceuticals, 790 Memorial Drive Suite 202, Cambridge, MA 02139.

<sup>§</sup>Current Address for Jaison Jacob: Wyeth Pharmaceuticals, 35 Cambridge Park Drive, Cambridge, MA 02140

Current Address for Alvira Slutsky: A.N. Bakh Institute of Biochemistry, Russian Academy of Sciences, Leninsky Pr. 33, Moscow, 117071, Russia

protein crosslinks<sup>14</sup> are also formed. The 3-(2-deoxy- $\beta$ -Derythro-pentofuranosyl)-5,6,7,8-tetrahydro-8-hydroxypyrimido[1,2a]purin-10(3H)-one,  $\gamma$ -OH-PdG adduct **2**<sup>1,9</sup> was detected in animal and human tissue,<sup>1</sup> suggesting its involvement in mutagenesis and carcinogenesis.<sup>15</sup> Methods for site-specific synthesis of **2** in oligodeoxynucleotides were developed.<sup>16,17</sup> When placed into duplex DNA opposite dC at neutral pH, **2** opened spontaneously to aldehyde **3**, in equilibrium with diol **3a**.<sup>18</sup>

The  $\gamma$ -OH-PdG adduct **2** was weakly mutagenic in *Escherichia coli*<sup>19</sup> and in HeLa, XP-A, and XP-V cells.<sup>20–22</sup> This was attributed<sup>19–21</sup> to its conversion to the ring-opened aldehyde **3** or the corresponding hydrated aldehyde **3a** in duplex DNA.<sup>18</sup> The stable analog of adduct **2**, 1,N<sup>2</sup>-propanodeoxyguanosine (PdG), induced G→T transversions and G→A transitions.<sup>23,24</sup> When adduct **2** was inserted into a single-stranded pMS2 vector<sup>25</sup> and replicated in COS-7 cells, conditions under which it was not expected to undergo ring-opening to aldehyde **3** or hydrated aldehyde **3a**, its mutagenic spectrum was similar to PdG.<sup>26</sup> Similarly, the regioisomeric  $\alpha$ -OH-PdG, which was stable as the cyclic adduct in duplex DNA, exhibited increased mutagenicity in human XP-A cells.<sup>22</sup> In COS-7 cells,  $\alpha$ -OH-PdG induced mutations at 8 % frequency.<sup>14</sup>

The presence of aldehyde **3** in duplex DNA leads to the potential for formation of both DNA-DNA and DNA-protein crosslinks. Kozekov et al.<sup>10,11</sup> trapped a trimethylene crosslink upon insertion of  $\gamma$ -OH-PdG adduct **2** into an oligodeoxynucleotide duplex at a 5'-CpG-3' sequence, followed by NaCNBH<sub>3</sub> treatment. This implied the presence of crosslinked imine **5**, in equilibrium with crosslinked carbinolamine **4**. Enzymatic digestion of the crosslinked DNA afforded crosslinked pyrimidopurinone **6**,<sup>10</sup> although it is not clear if the latter species is also in equilibrium with the carbinolamine and imine or if it is formed after the digestion. In contrast, <sup>15</sup>N HSQC NMR detected the presence of carbinolamine **4** *in situ*, in the 5'-CpG-3' sequence.<sup>12</sup> The interstrand carbinolamine **4**, imine **5**, and potentially, the pyrimidopurinone **6** crosslinks formed in 5'-CpG-3' sequences exist in equilibrium (Scheme 1) and monitoring the composition of the mixture *in situ* is of considerable interest. All three crosslinked species may contribute to the mutagenic spectrum of acrolein, and interfere with DNA replication.

Here we show that the site-specific introduction of a <sup>13</sup>C label at the  $\gamma$  carbon, and of a <sup>15</sup>N label at N<sup>2</sup>-dG of  $\gamma$ -OH-PdG, enables the equilibrium chemistry of  $\gamma$ -OH-PdG adduct **2** to be monitored, *in situ*. The results reveal that the previously detected<sup>12</sup> carbinolamine **4** is in fact the major cross-linked species present in duplex DNA, *in situ*. At equilibrium, the amounts of imine crosslink **5** and pyrimidopurinone crosslink **6** remain below the level of detection. Molecular modeling suggests carbinolamine crosslink **4** maintains Watson-Crick hydrogen bonding at both of the tandem C•G base pairs, with minimal distortion of the duplex.

## Experimental Section

### Materials and Methods

Chemicals obtained from commercial sources were of reagent grade. Methylene chloride was freshly distilled from calcium hydride. Anhydrous tetrahydrofuran (THF) was freshly distilled from a sodium/benzophenone ketyl. All reactions were performed under argon atmosphere in oven-dried glassware. Flash column chromatography was performed using silica gel (70–230 mesh). Oligodeoxynucleotides were purified by C-18 reversed phase HPLC in water/acetonitrile with a diode array detector monitoring at 260 nm using the following solvent gradient: the initial conditions was 99% water, then a 15 min linear gradient to 90% water, 5 min linear gradient to 80% water, 5 min at 80%, 10 min linear gradient to 20% water, and 5 min at 20% followed by 5 min linear gradient to initial conditions. MALDI-TOF mass spectra (negative ion) of modified oligodeoxynucleotides were obtained on a Voyager Elite DE instrument (Perseptive Biosystems) at the Vanderbilt Mass Spectrometry Resource Facility

using a 3-hydroxypicolinic acid (HPA) matrix containing ammonium hydrogen citrate (7 mg/mL) to suppress sodium and potassium adducts.  $^1\text{H}$  and  $^{13}\text{C}$  NMR data were recorded at 300 and 75 MHz or 400 MHz and 100 MHz (Bruker Instruments), respectively.

**Synthesis of  $^{13}\text{C}$ -Labeled  $\gamma$ -OH-PdG Adducted Oligodeoxynucleotide. (a) *tert*-butyl *N*-(2-Hydroxyethyl)carbamic acid (7)**

To a stirred solution of ethanolamine (0.611 g, 10 mmol) and 1N NaOH (10 mL) cooled to 0 °C, a solution of di-*tert*-butyldicarbonate (2.4 g, 11 mmol) in methylene chloride (30 mL) was added dropwise. The mixture was allowed to warm to room temperature, and vigorously stirred overnight. The layers were separated and the organic phase was successively washed with 0.1 N HCl, 5%  $\text{NaHCO}_3$  and brine, then dried over  $\text{MgSO}_4$ , filtered and concentrated. Purification by flash chromatography on silica gel, eluting with 2–3% methanol in chloroform, gave **7** (1.14 g, 70%):  $^1\text{H}$  NMR ( $\text{CDCl}_3$ )  $\delta$  5.02 (br, 1H), 3.70 (dd, 2H,  $J = 3.8, 7.7$  Hz), 3.29 (dd, 2H,  $J = 3.8, 7.7$  Hz), 2.66 (br, 1H), 1.45 (s, 9H).

**(b) *N*-*tert*-Butyl [2-( $^{13}\text{C}$ -cyano)ethyl]carbamic acid (8)**

To a stirred solution of **7** (386 mg, 2.4 mmol) and triethylamine (0.50 mL, 9.41 mmol, 3.6 mmol) in anhydrous methylene chloride (5 mL) cooled to 0 °C, was added a solution of methanesulfonyl chloride (310 mg, 2.64 mmol) in anhydrous methylene chloride (2 mL) dropwise. The reaction mixture was stirred at room temperature for 2 h then quenched with saturated  $\text{NaHCO}_3$  solution. The organic layer was separated, dried over  $\text{K}_2\text{CO}_3$ , filtered and concentrated under reduced pressure. The crude mesylate was dissolved in DMSO (10 mL) and  $\text{K}^{13}\text{CN}$  (237 mg, 3.6 mmol) was added in the solution. The solution was heated at 40 °C for 15 h then cooled to room temperature. Water (20 mL) was added to the solution and the mixture extracted with ether ( $3 \times 10$  mL). The combined organic extracts were washed with brine ( $3 \times 10$  mL), dried over  $\text{MgSO}_4$ , filtered, and concentrated under reduced pressure. Purification by flash chromatography on silica gel, eluting with 12–15% ethyl acetate in hexanes, gave **8** (288 mg, 70%):  $^1\text{H}$  NMR ( $\text{CDCl}_3$ )  $\delta$  5.01 (br, 1H), 3.40 (m, 2H), 2.60 (m, 2H), 1.45 (s, 9H).

**(c) *N*-(*tert*-butylcarbamoyl)-3-amino-1- $^{13}\text{C}$ -propanal (9)**

To a stirred solution of **8** (280 mg, 1.64 mmol) in anhydrous methylene chloride (5 mL) at  $-78^\circ\text{C}$  was added diisobutylaluminum hydride (1.0 M in methylene chloride, 4.1 mL) dropwise over 20 min. After the addition was complete, the reaction mixture was stirred at  $-78^\circ\text{C}$  for 10 min then quenched by the addition of acetone (1 mL), followed by saturated aqueous  $\text{NH}_4\text{Cl}$  (10 mL). The resulting mixture was allowed to warm to room temperature and stirred for 40 min. The mixture was filtered through a pad of celite and the filtrate washed with brine, dried over  $\text{MgSO}_4$ , filtered and evaporated under reduced pressure. Purification by flash chromatography on silica gel, eluting with 20–25% ethyl acetate in hexanes gave **9** (86 mg, 30.3%):  $^1\text{H}$  NMR ( $\text{CDCl}_3$ )  $\delta$  9.81 (d, 1H,  $J_{\text{C-H}} = 174$  Hz), 4.96 (br, 1H), 3.41 (m, 2H), 2.71 (m, 2H), 1.45 (s, 9H).

**(d) *N*-(*tert*-butylcarbamoyl)-4-amino-2- $^{13}\text{C}$ -but-1-ene (10)**

To a stirred suspension of methyltriphenylphosphonium bromide (206 mg, 0.576 mmol) in THF (5 mL) was added potassium *t*-butoxide in THF (1M in THF, 536  $\mu\text{L}$ , 0.536 mmol), and the reaction mixture was stirred for 30 min. The reaction mixture was cooled to 0 °C, and a solution of **9** (88 mg, 0.51 mmol) in THF (2 mL) was added. The reaction mixture was stirred for 1 h at room temperature then quenched with saturated aqueous  $\text{NH}_4\text{Cl}$  (10 mL) and the layers separated. The aqueous phase was extracted with ether ( $3 \times 10$  mL). The combined organic phases were dried over  $\text{Na}_2\text{SO}_4$ , filtered and evaporated under reduced pressure. Purification by flash chromatography on silica gel eluting with 3% ethyl acetate in hexanes

gave *N*-(*tert*-butylcarbonyl)-4-amino-2-<sup>13</sup>C-but-1-ene **10** (58 mg, 65.6%) as a colorless oil: <sup>1</sup>H NMR (CDCl<sub>3</sub>) δ 5.76 (m, J<sub>C-H</sub>=144 Hz, 1H), 4.45 (br, 1H), 3.01 (m, 2H), 2.24 (m, 2H), 1.45 (s, 9H).

**(e) *N*-(*tert*-butylcarbonyl)-3,4-dihydroxy-1-amino-3-<sup>13</sup>C-butane (**11**)**

To a stirred solution of *N*-(*tert*-butylcarbonyl)-4-amino-2-<sup>13</sup>C-but-1-ene **10** (45 mg, 0.26 mmol), *N*-methylmorpholine *N*-oxide (35 mg, 0.286 mmol), THF (0.8 mL), *t*-BuOH (0.32 mL), and water (0.16 mL) was added osmium tetroxide (10 μL, 0.1 M in benzene, 1.0 μmol). The mixture was stirred for 12 h and then a second portion of osmium tetroxide (6 μL, 0.1 M in benzene, 0.6 μmol) was added and stirring continued for an additional 8 h. The reaction was quenched by the addition of 5% aqueous NaHSO<sub>3</sub> (5 mL) and vigorous stirring for 15 min then poured over water. The layers were separated and the aqueous phase extracted with methylene chloride (10 × 3 mL). The combined organic extracts were dried over Na<sub>2</sub>SO<sub>4</sub>, filtered and concentrated under reduced pressure. Purification by flash chromatography on silica gel, eluting with 1–2% methanol in chloroform gave **11** (37 mg, 69.0%) as an inseparable mixture of diastereomers: <sup>1</sup>H NMR (CDCl<sub>3</sub>) δ 4.65–4.50 (br, 1H), 3.70 (m, J<sub>C-H</sub> = 135 Hz, 1H), 3.60 (m, 2H), 2.92 (m, 2H), 3.1 (m, 1H), 2.4 (m, 1H), 1.5 (m, 2H), 1.45 (s, 9H).

**(f) 4-Amino-2-<sup>13</sup>C-butane-1,2-diol (**12**)**

To a solution of **11** (30 mg, 0.145 mmol) in methylene chloride (1.5 mL) and methanol (0.5 mL) was added clean H-Amberlyst 15 resin (0.3 g).<sup>27</sup> The mixture was gently shaken for 14 h, after which time TLC showed that **11** had been consumed. The resin was removed by filtration and successively washed with THF and methanol. This amine-bound resin was transferred to a 4 M solution of ammonia in methanol and was gently shaken for 50 min. To this mixture was added methanol (3 × 5 mL) in order to dissolve all of the deprotected amine. The resin was then removed by filtration and the filtrate evaporated under reduced pressure to give **12** (14 mg, 91%), which was used without further purification. <sup>1</sup>H NMR (CD<sub>3</sub>OD) δ 3.73 (m, J<sub>C-H</sub> = 135 Hz, 1H), 3.45 (m, 2H), 2.84 (m, 2H), 1.6, (m, 1H) 1.5 (m, 1H).

**Synthesis of γ-<sup>13</sup>C-PdG-Modified Oligodeoxynucleotide 5'-GCTAGCXAGTCC-3' (**18**)**

The *O*<sup>6</sup>-trimethylsilylethane-2-fluorinosine-modified oligodeoxynucleotide<sup>34</sup> **16** (100 A<sub>260</sub> units) was mixed in a plastic test tube with diisopropylethylamine (150 μL), DMSO (500 μL), and 4-amino-2-<sup>13</sup>C-butane-1,2-diol **12** (6 mg). The reaction mixture was stirred at 55 °C for 24 h. The solvents were evaporated under vacuum with a centrifugal evaporator and the residue was dissolved in 5% acetic acid (500 μL) and stirred for 2 h at room temperature to remove the *O*<sup>6</sup>-trimethylsilylethane group. The mixture was neutralized with 1 M NaOH and purified by HPLC to give the corresponding *N*<sup>2</sup>-(3-<sup>13</sup>C-3,4-dihydroxybutyl)guanine-modified oligodeoxynucleotide **17** (68.7 OD – 68%). MALDI-TOF MS: calcd for [M – H]<sup>–</sup> 3733.7, found 3735.9.

An aqueous solution of NaIO<sub>4</sub> (500 μL, 20 mM) was added to a solution of *N*<sup>2</sup>-(3-<sup>13</sup>C-3,4-dihydroxybutyl)guanine-modified oligodeoxynucleotide **17** (68.6 A<sub>260</sub> units) in 0.05 M, pH 7.0 phosphate buffer, (2 mL) and the reaction mixture was stirred at room temperature for 10 min. The mixture was purified by HPLC to give 8-<sup>13</sup>C-8-hydroxy-5,6,7,8-tetrahydropyrimido [1,2-*a*]purin-10(3*H*)-one adducted oligodeoxynucleotide **18**. (63.7 OD - 93%) MALDI-TOF MS: calcd for [M – H]<sup>–</sup> 3701.6, found 3701.6.

**2-[2-(4*S*)-(2,2-Dimethyl-[1,3]dioxolan-4-yl)ethyl]-(1*H*)-2-<sup>15</sup>N-isoindole-1,3(2*H*)-dione (**14**)**

A stirred solution of (*4R*)-4-(2-hydroxyethyl)-2,2-dimethyl-1,3-dioxalane (**13**, 293 mg, 2 mmol) and triethylamine (0.34 mL, 2.4 mmol) in anhydrous CH<sub>2</sub>Cl<sub>2</sub> (8 mL) was cooled to 0 °C and then a solution of methanesulfonyl chloride (275 mg, 2.4 mmol) in anhydrous

CH<sub>2</sub>Cl<sub>2</sub> (2 mL) was added dropwise. The reaction mixture was allowed to warm to room temperature and stirred for 2 h. The reaction mixture was transferred to a separatory funnel and washed with saturated NaHCO<sub>3</sub> solution. The organic layer was dried over K<sub>2</sub>CO<sub>3</sub>, filtered and concentrated *in vacuo*. The crude mesylate and potassium phthalimide-<sup>15</sup>N (373 mg, 2mmol, dried in the oven) were dissolved in dry DMF (20 mL) and the reaction mixture heated at 65 °C overnight. After cooling at room temperature, the solvent was evaporated under high vacuum. Water (20 mL) was added, and the mixture was extracted with CH<sub>2</sub>Cl<sub>2</sub> (3 × 10 mL). The combined organic phases were washed with saturated brine (3 × 10 mL), dried over MgSO<sub>4</sub>, filtered, and concentrated *in vacuo*. Flash chromatography on silica gel, eluting with 5–8% EtOAc in hexane, gave **14** (300 mg, 54%): <sup>1</sup>H NMR (CDCl<sub>3</sub>) δ 7.84–7.69 (m, 4H), 4.12 (m, 1H), 4.06 (dd, J=7.5 and 6 Hz, 1H), 3.82 (m, 2H), 3.56 (dd, J=7.5 and 6.6 Hz, 1H), 1.92 (m, 2H), 1.35(s, 3H), 1.29(s, 3H).<sup>28</sup>

#### (2S)-4-<sup>15</sup>N-Amino-butane-1,2-diol (**15**)

A solution of **14** (132 mg, 0.48 mmol) and anhydrous N<sub>2</sub>H<sub>4</sub> (46 mg, 1.43 mmol) in absolute EtOH (3 mL) was heated under reflux for 2 h. Upon cooling to room temperature, a white solid precipitate formed, which was removed by filtration. The filtrate was cooled to 0° C and 2N HCl (1 mL) was added. The mixture was stirred for 1 h, and then filtered. The solvent and water were removed *in vacuo*. The residue was diluted with MeOH (5 mL), Dowex-H 50W resin (0.5 g) was added and the suspension was shaken for 10 h. The resin was then removed by filtration and successively washed with THF and MeOH. This amine-bound resin was suspended in a 4 M ammonia in methanol solution and gently shaken for 50 min. The resin was then removed by filtration and washed with MeOH (3 × 5 mL). The combined filtrates were then evaporated to give **15** (30 mg, 59%): <sup>1</sup>H NMR (CD<sub>3</sub>OD) δ 3.61(m, 1H), 3.46 (m, 2H), 2.86 (m, 2H), 1.7–1.5 (m, 2H).<sup>17</sup>

#### Synthesis of γ-OH-<sup>15</sup>N<sup>2</sup>-PdG-Modified Oligodeoxynucleotide 5'-GCTAGCXAGTCC-3' (**20**)

The O<sup>6</sup>-trimethylsilylethane-2-fluorinosine-modified oligodeoxynucleotide<sup>34</sup> **16** (80 A<sub>260</sub> units) was mixed in a plastic test tube with diisopropylethylamine (200 μl), DMSO (500 μl), and **15** (8 mg). The reaction mixture was stirred at 60° C for 7 h. HPLC analysis showed complete disappearance of the starting oligodeoxynucleotide. The solvents were removed *in vacuo* using a centrifugal evaporator. The residue was dissolved in 5% acetic acid (1 mL) and the mixture stirred for 2 h at room temperature. The mixture was neutralized with 1 M NaOH and purified by HPLC to yield the corresponding modified oligodeoxynucleotide **19** (65 A<sub>260</sub> units, ~81 %). MALDI-TOF-MS: *m/z* calcd for 3733.7, found 3733.6. A solution of NaIO<sub>4</sub> (100 mL, 20 mM) was added to a solution of modified oligodeoxynucleotide **19** (~65 A<sub>260</sub> units) in phosphate buffer (pH 7, 0.05M, 0.4 mL). The reaction mixture was stirred at room temperature for 1 h and then was purified by HPLC to give oligodeoxynucleotide **20** (52 A<sub>260</sub> units, 80%). MALDI-TOF-MS: *m/z* calcd for 3701.6, found 3701.9.

#### Synthesis of <sup>15</sup>N<sup>2</sup>-dG-Modified Oligodeoxynucleotide 5'-GGACTCXCTAGC-3' (**22**)

The O<sup>6</sup>-trimethylsilylethane-2-fluorinosine-modified oligodeoxynucleotide<sup>34</sup> **21** was deprotected using 6 M <sup>15</sup>NH<sub>4</sub>OH, and desilylated with 5 % acetic acid, and purified by C8 HPLC in 0.1 M ammonium formate (pH 6.5), yielding <sup>15</sup>N<sup>2</sup>-dG-modified oligodeoxynucleotide **22**. Negative ion MALDI-TOF mass spectrometry yielded *m/z* 3645.9 (calcd for [M–H]<sup>–</sup> 3645.6).

#### Oligodeoxynucleotide Characterization

The concentrations of the single-stranded oligodeoxynucleotides were determined from calculated extinction coefficients at 260 nm.<sup>29</sup> The purities of the modified oligodeoxynucleotides were analyzed using a PACE 5500 capillary electrophoresis (Beckman

Instruments, Inc., Fullerton, CA) instrument. Electrophoresis was conducted using an eCAP ssDNA 100-R kit applying 12,000 V for 30 min. The electropherogram was monitored at 254 nm. MALDI-TOF mass spectra were measured on a Voyager-DE (PerSeptive Biosystems, Inc., Foster City, CA) instrument in negative reflector mode. The matrix contained 0.5 M 3-hydroxypicolinic acid and 0.1 M ammonium citrate. The modified duplex oligodeoxynucleotides were eluted from DNA Grade Biogel hydroxylapatite (Bio-Rad Laboratories, Hercules, CA) with a gradient from 10 to 200 mM Na<sub>2</sub>HPO<sub>4</sub> (pH 7.0). They were desalted using Sephadex G-25. For NMR studies, the  $\gamma$ -OH-PdG-modified oligodeoxynucleotide duplexes 5'-d(GCTAGCXAGTCC)-3'•5'-d(GGACTCYCTAGC)-3' (X= $\gamma$ -OH-PdG; Y=dC, T, or dA) were annealed in a buffer consisting of 10 mM Na<sub>2</sub>HPO<sub>4</sub>, 0.1 M NaCl, and 50  $\mu$ M Na<sub>2</sub>EDTA (pH 7.0).

## NMR

The duplex oligodeoxynucleotides were prepared at a concentration of 2 mM in 0.3 mL of 9:1 H<sub>2</sub>O:D<sub>2</sub>O containing 10 mM NaH<sub>2</sub>PO<sub>4</sub>, 0.1 M NaCl, and 50  $\mu$ M Na<sub>2</sub>EDTA (pH 7.0). They were placed into micro-NMR tubes (Shigemi Glass, Inc., Allison Park, PA). The NMR experiments were carried out at <sup>1</sup>H frequencies of 500.13 or 600.13 MHz (<sup>13</sup>C frequencies of 125 or 150 MHz; <sup>15</sup>N frequencies of 50.66 or 60.79 MHz). One-dimensional <sup>13</sup>C NMR was conducted with a probe with inner-coil <sup>13</sup>C geometry using inverse-gated <sup>1</sup>H WALTZ16 decoupling. Typical acquisition parameters were 16 K total data points, with a digital resolution of 1.3 Hz/pt, 12K scans, and a relaxation delay of 8 s. The <sup>13</sup>C HSQC experiments were performed using standard <sup>1</sup>H-detected pulse programs with States-TPPI phase cycling and watergate water suppression.<sup>30</sup> Typical experimental parameters were 8 scans, 512 FIDs, each of 2K points. The <sup>13</sup>C sweep width was varied from 20 to 180 ppm. The <sup>15</sup>N NOESY-HSQC<sup>31,32</sup> experiments were recorded by application of States phase cycling, with a 150 ms mixing time, and were optimized for a 90 Hz <sup>1</sup>J<sub>N-H</sub> coupling. There were total of 2048 complex data points covering 10,000 Hz in the acquisition dimension, and 128 points centered at 80 ppm in the indirect dimension and covering 1,000 Hz. A relaxation delay of 1.5 sec was used, and <sup>15</sup>N was decoupled during the acquisition time. The <sup>1</sup>H chemical shifts were referenced to water. Both <sup>13</sup>C and <sup>15</sup>N chemical shifts were referenced indirectly.<sup>33–35</sup> The NMR data were processed on Silicon Graphics Octane workstations using the programs FELIX2000 (Accelrys, Inc., San Diego, CA) or NMRPipe.<sup>36</sup>

## Trapping of DNA–Peptide Complexes

A (non-isotopically-labeled) modified 12-mer oligodeoxynucleotide<sup>17</sup> was ligated with the 5'- and 3'-flanking oligodeoxynucleotides as previously described,<sup>26</sup> yielding the 58-mer 5'-CGTCGCCAGCTGGCCACCCCTGCTAGCXAGTCCGCGCCAAGTTTGGGCTGCAGCAGGT C-3'; X=  $\gamma$ -OH-PdG. The modified oligodeoxynucleotide was 5'-<sup>32</sup>P-labeled with T4 polynucleotide kinase (New England BioLabs, Beverly, MA) and annealed to complementary oligodeoxynucleotides following standard protocols. Formation of duplex DNA was confirmed by polyacrylamide gel electrophoresis (PAGE) under native conditions. The tetrapeptide KWKK was obtained from Sigma-Genosys (Woodlands, TX). It was reconstituted in 20% (v/v) acetonitrile (Sigma, St. Louis, MO) and stored as 10 mM solution at -20 °C. Modified oligodeoxynucleotides (2 nM) were incubated with KWKK (100  $\mu$ M) in 100 mM Hepes-Na (pH 7.0) in the presence of 25 mM NaCNBH<sub>3</sub> (Sigma, St. Louis, MO) at 22 °C. Reactions were terminated by the addition of two volumes of the DNA denaturing solution [95% (v/v) formamide, 20 mM EDTA, 0.2% (w/v) bromphenol blue, 0.2% (w/v) xylene cyanol] followed by the heating at 90 °C for 5 min. DNA samples were immediately frozen and stored at -20 °C prior to separation by denaturing PAGE (in the presence of 8 M urea). Results were visualized by PhosphorImager analysis. Quantifications were performed using ImageQuant (v. 5.2) software.

## Molecular Modeling

Modeling was performed on Silicon Graphics Octane workstations using the program AMBER 8.0.<sup>37</sup> Classical B-DNA was used as a reference structure to create starting structures for potential energy minimization.<sup>38</sup> Diastereomers of carbinolamine crosslink **4** and pyrimidopurinone crosslink **5** were constructed using the BUILDER module of INSIGHT II (Accelrys, Inc., San Diego, CA). The program ANTECHAMBER was used, and the atom types were based on AMBER atom types for parameterization. RESP atomic charges were calculated using GAUSSIAN98<sup>39</sup> and the Hartree-Fock 6-31G\* basis set. The generalized Born model for solvent<sup>40,41</sup> was utilized for potential energy minimization. Potential energy minimization used the AMBER 8.0 force field.

## Results

### Site-Specific Synthesis of <sup>13</sup>C and <sup>15</sup>N Labeled $\gamma$ -OH-<sup>13</sup>C-PdG Oligodeoxynucleotides

The synthesis of the <sup>13</sup>C- and <sup>15</sup>N-labeled adducted oligodeoxynucleotides was accomplished using a post-oligomerization strategy previously employed for related modified oligodeoxynucleotides.<sup>10,42</sup> This involved the incorporation of an electrophilic base, 2-fluoro-*O*<sup>6</sup>-(2-trimethylsilylethyl)-2'-deoxyinosine,<sup>43</sup> into an oligodeoxynucleotide using standard phosphoramidite chemistry followed by displacement of the fluoro group by an amine analogue of the mutagen via a nucleophilic aromatic substitution reaction. A vicinal diol unit was used as a surrogate for the aldehyde group, which was cleaved with sodium periodate after the adduction reaction to give the desired modified oligodeoxynucleotide. The synthesis of the <sup>13</sup>C- and <sup>15</sup>N-labeled amino diols **12** and **15** is shown in Scheme 2 and Scheme 3.

The synthesis of the <sup>13</sup>C-labeled amino diol **12** began with the conversion of alcohol **7** to the corresponding mesylate followed by displacement with <sup>13</sup>C-labelled potassium cyanide (Scheme 2). Reduction of the nitrile **8** with DiBAL-H at low temperature followed by hydrolysis gave the labeled aldehyde **9**. Wittig olefination followed by treatment with osmium tetroxide installed the vicinal diol unit. Deprotection of the amino group then provided the desired amino diol **12** with the <sup>13</sup>C-label in the proper location.<sup>27</sup>

The synthesis of the <sup>15</sup>N-labeled 4-aminobutane-1,2-diol **15** is outlined in Scheme 3. The hydroxyl group of alcohol **13** was converted to the corresponding mesylate, which was displaced by potassium <sup>15</sup>N-phthalimide in DMF. Treatment with hydrazine and purification by ion-exchange chromatography gave the desired <sup>15</sup>N-labeled substrate **15**.

The specifically labeled adducted oligodeoxynucleotides (**18** and **20**) were prepared according to Scheme 4. Reaction of oligodeoxynucleotide **16** containing the 2-fluoro-*O*<sup>6</sup>-(2-trimethylsilylethyl)-2'-deoxyinosine with either the <sup>13</sup>C- or <sup>15</sup>N-labeled aminodiol **12** or **15** under nucleophilic aromatic substitution conditions gave specifically adducted oligodeoxynucleotide **17** or **19**. Periodate oxidation of the vicinal diol unit gave the corresponding aldehyde, which exists in the ring-closed form **18** and **20** in single-stranded DNA.

The site-specific incorporation of an <sup>15</sup>N<sup>2</sup>-dG label in the complementary strand involved the incorporation of the 2-fluoro-*O*<sup>6</sup>-(2-trimethylsilylethyl)-2'-deoxyinosine nucleotide into the desired position using phosphoramidite chemistry.<sup>10,11,43,44</sup> This oligodeoxynucleotide was then deprotected using 6M <sup>15</sup>NH<sub>4</sub>OH which also displaced the fluoro group. Removal of the *O*<sup>6</sup>-(2-trimethylsilylethyl) protecting group using 5% acetic acid afforded the site-specifically <sup>15</sup>N-labeled oligodeoxynucleotide **22**.

### Epimerization of $\gamma$ -OH-PdG

The single-stranded 5'-d(GCTAGCXAGTCC)-3'  $\gamma$ - $^{13}\text{C}$ -OH-PdG oligodeoxynucleotide **18** was examined using  $^{13}\text{C}$  HSQC NMR (Figure 1). At 37 °C two  $\gamma$ - $^{13}\text{C}$  resonances were observed at  $\delta$  71.3 ppm. The corresponding  $^1\text{H}$  resonances were observed at  $\delta$  6.12 and 6.01 ppm. These two resonances were assigned as the *R*- and *S*-epimers of cyclic adduct **2**, embedded in oligodeoxynucleotide **18**. No resonance for  $\gamma$ - $^{13}\text{C}$  aldehyde **3** or hydrated aldehyde **3a** was observed, suggesting that at equilibrium, the levels of these ring-opened species remained below the spectroscopic limit of detection.

### Equilibrium Chemistry of the $\gamma$ -OH-PdG Adduct in Duplex DNA

The single-stranded 5'-d(GCTAGCXAGTCC)-3'  $\gamma$ - $^{13}\text{C}$ -OH-PdG oligodeoxynucleotide **18** was annealed with the complementary strand to form the duplex 5'-d(GCTAGCXAGTCC)-3'•5'-d(GGACTCGCTAGC)-3' at pH 7, in which adduct **2** was placed opposite dC, and the sample was allowed to equilibrate at 37 °C (Figure 2). After 6 days, no further spectroscopic changes were observed. At equilibrium, the  $\gamma$ - $^{13}\text{C}$  resonance in oligodeoxynucleotide **18** appeared as a mixture of three species. Furthest downfield, at approximately 207 ppm, was a resonance assigned as  $\gamma$ - $^{13}\text{C}$  aldehyde **3**. A second  $\gamma$ - $^{13}\text{C}$  resonance, assigned as hydrated aldehyde **3a**,<sup>45</sup> was observed at approximately 90 ppm. The third resonance, assigned as carbinolamine crosslink **4**, was observed at 76 ppm. The two diastereomers of carbinolamine **4** were not resolvable in the  $^{13}\text{C}$  spectrum. The secure assignment of the crosslinked resonance as carbinolamine **4** and not pyrimidopurinone **6** was accomplished by annealing  $^{15}\text{N}$ -labeled oligodeoxynucleotide **20** with the complementary strand at pH 7. An  $^{15}\text{N}$ -HSQC filtered NOESY spectrum revealed the presence of an NOE between X<sup>7</sup>  $^{15}\text{N}^2\text{H}$  and the imino proton X<sup>7</sup>  $\text{NH}$ , which was not consistent with the presence of pyrimidopurinone **6** (Figure 3). Supporting evidence for the assignment of carbinolamine **4** was derived from a triple resonance HCN experiment conducted subsequent to annealing  $^{13}\text{C}$ -labeled oligodeoxynucleotide **18** with  $^{15}\text{N}$ -labeled complement **22** (data not shown). Crosslink formation resulted in bonding between the  $^{15}\text{N}$  and  $^{13}\text{C}$  isotopes. A correlation was observed between the 76 ppm  $\gamma$ - $^{13}\text{C}$  resonance and a  $^{15}\text{N}$  resonance at 106 ppm, establishing that crosslink **4** observed in the  $^{13}\text{C}$  experiments (Figure 2) arose from the same chemical species observed in  $^{15}\text{N}$  HSQC experiments, and assigned as carbinolamine **4**.<sup>12</sup> The ~5 ppm  $^{13}\text{C}$  chemical shift difference of carbinolamine **4** as compared to cyclic adduct **2** was consistent with the expectation that the  $\gamma$ - $^{13}\text{C}$  nuclei in adducts **2** and **4**, both of which were bonded to hydroxyl groups, should exhibit similar chemical shifts.

### Rate of Interstrand Crosslink Formation

An inverse-gated  $^{13}\text{C}$  spectrum was obtained immediately upon annealing  $^{13}\text{C}$ -labeled oligodeoxynucleotide **18** with its complement. The  $\gamma$ - $^{13}\text{C}$  resonances from aldehyde **3** and hydrated aldehyde **3a** were detected, indicating that opening of adduct **2** was complete before the  $^{13}\text{C}$  spectrum could be collected. The  $\gamma$ - $^{13}\text{C}$  resonance assigned as carbinolamine crosslink **4** was observed as a weak signal in the day 1 spectrum. It increased in intensity over a period of 6 days at 37 °C. The failure to observe a  $\gamma$ - $^{13}\text{C}$  resonance in the 140–160 ppm spectral region, the range in which a resonance arising from  $\gamma$ - $^{13}\text{C}$  imine **5** would be anticipated, indicated that the amount of imine **5** in equilibrium with carbinolamine **4** was below the level of detection by  $^{13}\text{C}$  NMR. This placed an upper limit on the amount of imine crosslink **5** in equilibrium with carbinolamine crosslink **4**, estimated to be  $\leq 5\%$ . At longer acquisition times, the natural abundance  $^{13}\text{C}$  spectrum of the duplex oligodeoxynucleotide was observed.

Figure 4 shows the inverse-gated  $^{13}\text{C}$  spectrum of the equilibrated sample as a function of temperature. At lower temperature, the intensity of the resonance arising from hydrated aldehyde **3a** increased, concomitant with a decrease in intensity of the resonance arising from aldehyde **3**. At 37 °C, a 1:1 aldehyde **3**:hydrated aldehyde **3a** ratio was observed, while a 1:2



ratio of aldehyde to hydrated aldehyde (**3:3a**) was observed at 25 °C. Below the  $T_m$  of the duplex, the integrated area of the resonance arising from carbinolamine crosslink **4** did not vary. It did, however, undergo line broadening as temperature was lowered. Above 65 °C thermal denaturation of the duplex oligodeoxynucleotide occurred and only the resonance arising from cyclic adduct **2** was observed. No resonance arising from a transiently formed  $\gamma$ - $^{13}\text{C}$  imine **5** was detected through this range of temperature.

### Mispairing of T and dA Opposite the $\gamma$ -OH-PdG Adduct

The acrolein  $\gamma$ - $^{13}\text{C}$ -OH-PdG adducted oligodeoxynucleotide **18** was annealed with the mismatched oligodeoxynucleotides placing a T opposite adduct **2** in 5'-d(GCTAGCXAGTCC)-3'•5'-d(GGACTTGCTAGC)-3', and placing dA opposite adduct **2** in 5'-d(GCTAGCXAGTCC)-3'•5'-d(GGACTAGCTAGC)-3', at pH 7. The degree of ring-opening to aldehyde **3** and hydrated aldehyde **3a** was monitored by  $^{13}\text{C}$  NMR (Figure 5). When placed opposite T, at equilibrium, an equilibrium mixture of aldehyde **3**, hydrated aldehyde **3a**, and cyclic adduct **2**, was observed. When placed opposite dA, no opening of cyclic adduct **2** was observed.

### Formation of DNA–Peptide Complexes by the $\gamma$ -OH-PdG Adduct Placed Opposite to T and dA

Borohydride trapping probed for the presence of aldehyde **3** in the mismatched duplex DNAs containing either dA or T opposite to cyclic adduct **2**. The single-strand oligodeoxynucleotide containing adduct **2** was assayed as a reference. The 58-mer DNAs containing adduct **2** were incubated with KWKK tetrapeptide in the presence of  $\text{NaCNBH}_3$ , and accumulation of the trapped DNA–peptide complexes was monitored using PAGE (Figure 6). In agreement with previous results,<sup>13</sup> when adduct **2** correctly paired with dC, it efficiently formed DNA–peptide complexes (data not shown). In reactions with single-stranded DNA, accumulation of DNA–peptide complexes was low (Figure 5).<sup>13</sup> When adduct **2** was mispaired with T or dA, it also formed DNA–peptide complexes, albeit with different efficiencies. Specifically, initial rates of peptide crosslink formation were 1.64, 0.14, and 0.27  $\text{fmol}\cdot\text{min}^{-1}$  when cyclic adduct **2** was mismatched opposite T, dA, or in single-stranded DNA, respectively.

### Thermal Stability of the Interstrand Crosslink

$^{15}\text{N}$ -labeled oligodeoxynucleotide **22** was annealed with the complementary adducted oligodeoxynucleotide. A  $^{15}\text{N}$ -NOESY-HSQC experiment<sup>31,32</sup> revealed that the 5' C•G base pair of the crosslink maintained Watson–Crick hydrogen bonding,<sup>12</sup> which as will be discussed below, was consistent with molecular modeling of carbinolamine **4**. The  $T_m$  of the crosslinked duplex increased to 90 °C,<sup>10</sup> in support of the molecular modeling studies and suggesting that carbinolamine **4** stabilized the duplex with respect to thermal denaturation.

### Molecular Modeling

Two diastereomers of the 5'-CpG-3' carbinolamine interstrand crosslink **4** were modeled and compared to the corresponding unmodified oligodeoxynucleotide sequence. The model structures were subjected to potential energy minimization using the conjugate gradients algorithm in AMBER 8.0 (Figure 7). The potential energy minimization predicted that both diastereomers of carbinolamine crosslink **4** maintained Watson–Crick hydrogen bonding at both of the tandem C•G base pairs involved in the interstrand crosslinks. The modeling studies suggested that the  $\text{sp}^3$  hybridization at the  $\gamma$ -carbon of the acrolein moieties allowed the crosslinks to form without substantial perturbation of duplex structure. For the *S*-diastereomer of the carbinolamine crosslink, the molecular modeling predicted the possibility of an additional hydrogen bond between the carbinolamine hydroxyl and  $\text{N}^3$ -dG of the 5' C•G base pair of the crosslink. In contrast, imine **5** mandated  $\text{sp}^2$  hybridization at the  $\gamma$ -carbon of the

crosslink, which would require breaking the Watson-Crick hydrogen bond between the amine proton of N<sup>2</sup>-dG and O<sup>2</sup>-dC of the 5' C•G base pair in the crosslink. The modeling suggested that formation of either diastereomer of pyrimidopurinone crosslink **6** prevented Watson-Crick hydrogen bonding at the 3' G•C base pair of the crosslink. It suggested disrupted Watson-Crick hydrogen bonding at the 5' C•G base pair of the crosslink, which, as noted above, was not consistent with <sup>15</sup>N-NOESY-HSQC NMR experiments revealing that the 5' C•G base pair of the crosslink was intact.<sup>12</sup> The parameterization of the carbinolamine and the pyrimidopurinone crosslinks, for the AMBER 8.0 forcefield, is provided in the Supporting Information.

## Discussion

### Epimerization of the $\gamma$ -OH-PdG Adduct in the 5'-CpG-3' Sequence

In single-stranded DNA,  $\gamma$ -OH-PdG adduct **2** existed as an equal mixture of two epimers. This suggested that in this 5'-CpXpA-3' single-stranded DNA sequence the two configurations of the  $\gamma$ -hydroxyl group were equally favored energetically. This was consistent with the notion that in the single-stranded DNA, there was little steric hindrance to either configuration due to the fact that the 1,N<sup>2</sup>-cyclic ring faced away from the phosphodiester backbone. This contrasted with the situation in duplex DNA, in which the 1,N<sup>2</sup>-cyclic ring of adduct **2** clashed sterically with its complement and disrupted Watson-Crick hydrogen bonding. The failure to observe a  $\gamma$ -<sup>13</sup>C resonance corresponding to ring-opened aldehyde **3** in single-stranded DNA was consistent with the observation that at pH 7, cyclic adduct **2** was favored as compared to ring-opened aldehyde **3**. The data suggested that in single-stranded DNA, adduct **2** spontaneously epimerizes, but slowly on the NMR time scale, without accumulation of aldehyde **3**.

### Ring Opening of the $\gamma$ -OH-PdG Adduct in the 5'-CpG-3' Sequence

When placed into duplex DNA at pH 7 and 37 °C, with dC opposite  $\gamma$ -OH-PdG adduct **2**, ring-opening yielded approximately equal amounts of aldehyde **3** and hydrated aldehyde **3a**. De los Santos et al. reported two resonances for the H <sub>$\gamma$</sub>  proton of the ring-opened adduct, resonating at  $\delta$  9.58 ppm and  $\delta$  4.93 ppm, assigned as aldehyde **3** and hydrated aldehyde **3a**.<sup>18</sup> The equilibrium ratio of aldehyde to hydrated aldehyde (**3**:**3a**) increased with temperature, consistent with expectation. The presence of significant levels of aldehyde **3** in the minor groove at pH 7 and 37 °C was significant with regard to its propensity for forming crosslinks **4** under physiological conditions.

### The Interstrand Crosslink Exists as a Carbinolamine, *in situ*

It had been concluded that the interstrand acrolein crosslink must be comprised of an equilibrium mixture of carbinolamine **4**, imine **5**, and pyrimidopurinone **6**. Carbinolamine **4** was detected by <sup>15</sup>N HSQC NMR<sup>12</sup> and the presence of imine **5** was inferred because the crosslink was reductively trapped in the presence of NaCNBH<sub>3</sub>.<sup>10,11</sup> The present NMR studies suggest that the predominant form of the acrolein crosslink *in situ*, is in fact, carbinolamine **4**. The amount of imine **5** remained below the level of spectroscopic detection. Since the overall rate of the reduction of the interstrand crosslink occurred slowly in the presence of NaCNBH<sub>3</sub>,<sup>10,11</sup> these data suggest that dehydration of carbinolamine **4** to the reducible imine **5** is rate limiting in duplex DNA. Enzymatic digestion of duplex DNA containing crosslink **4** afforded a bis-deoxyguanosine conjugate, characterized by NMR as pyrimidopurinone **6** arising from annelation of imine **5** with N1-dG in the 5'-CpG-3' sequence.<sup>10</sup> The likely explanation is that the position of the equilibrium between carbinolamine **4**, imine **5**, and pyrimidopurinone **6** depends upon the conformational state of the DNA. Upon enzymatic degradation of duplex DNA, the equilibrium shifts to favor the pyrimidopurinone bis-nucleoside crosslink **6**. The time required for crosslink **4** to reach equilibrium at pH 7 and 37 °C was approximately 6 days, with approximately 40% crosslinking observed. These results

corroborated studies in which the interstrand crosslinking reaction was monitored by reverse-phase HPLC with gradient elution, using acetonitrile. In those studies, equilibrium was reached within 7 days, and crosslink **4** was present at a level of approximately 50%.<sup>10</sup>

### The DNA Duplex Maintains the Interstrand Carbinolamine Crosslink

Molecular modeling provided a rationale as to why the carbinolamine interstrand crosslink **4** predominated, *in situ*. It was predicted to conserve Watson-Crick hydrogen bonding at both of the tandem C•G base pairs, with minimal structural perturbation of the DNA duplex (Figure 7). The carbinolamine linkage maintained the N<sup>2</sup>-dG amine proton, necessary for maintaining Watson-Crick hydrogen bonding at the 5'-side of the interstrand crosslink. In addition, the carbinolamine hydroxyl group was predicted to be positioned such that it could allow an additional hydrogen bond at the 5'-side of the interstrand crosslink. This provided an explanation both as to why elimination of water to form the reducible imine **5** was slow in duplex DNA and why the reversible 5'-CpG-3' crosslink was extraordinarily stable with respect to thermal denaturation.<sup>10</sup> Thus, the formation of imine **5** was predicted to require disruption of Watson-Crick hydrogen bonding at both tandem C•G base pairs, whereas thermal strand dissociation to release the interstrand crosslink, required breaking possibly an additional hydrogen bond at the 5'-side of the interstrand crosslink. This was consistent with observations that oligodeoxynucleotides containing crosslink **4**, once isolated, were relatively stable under conditions that maintained duplex DNA structure. However, they reverted completely to the single-stranded oligodeoxynucleotides within 1 h in unbuffered H<sub>2</sub>O, conditions that favored duplex denaturation.<sup>11</sup> The molecular modeling predicted that formation of pyrimidopurinone crosslink **6** in duplex DNA required disruption of Watson-Crick hydrogen bonding at both tandem C•G base pairs. It resulted in a distorted conformation of the duplex, which was not consistent with the thermal stabilization of the duplex DNA afforded by the crosslink.

### Mispairing of the $\gamma$ -OH-PdG Adduct

In the nucleoside, or in the single-stranded oligodeoxynucleotide, equilibrium between cyclic adduct **2** and the ring-opened aldehyde **3** or hydrated aldehyde **3a** adducts favored adduct **2** at neutral pH (Figure 1); under basic conditions ring-opening was favored.<sup>18</sup> In duplex DNA, when adduct **2** was placed opposite dC at neutral pH, opening of adduct **2** to the aldehyde **3** or hydrated aldehyde **3a** adducts was favored,<sup>18</sup> and, *vide infra* (Figure 2). It is thought that when paired opposite dC at neutral pH, the equilibrium shifts because the aldehyde **3** or hydrated aldehyde **3a** adducts orient into the minor groove, conserving Watson-Crick hydrogen bonding.<sup>18</sup>

Chemically,  $\gamma$ -OH-PdG adduct **2** is similar to the pyrimidopurinone M<sub>1</sub>dG adduct formed in DNA upon exposure to malondialdehyde<sup>46–50</sup> or base propenals.<sup>51</sup> When placed into duplex DNA opposite dC at neutral pH, M<sub>1</sub>dG spontaneously opened to N<sup>2</sup>-(3-oxopropenyl)-dG (OpdG).<sup>52</sup> Similar to  $\gamma$ -OH-PdG adduct **2**, it is thought that when paired opposite dC at neutral pH, the equilibrium between M<sub>1</sub>dG and OPdG favors the latter, because it orients into the minor groove, conserving Watson-Crick hydrogen bonding.<sup>52,53</sup> However, in duplex DNA, the rate at which M<sub>1</sub>dG converted to OPdG was negligible unless M<sub>1</sub>dG was opposite dC in the complementary strand. When M<sub>1</sub>dG was placed opposite T, rather than dC, OPdG did not form at a measurable rate, although OPdG itself was stable opposite T.<sup>52</sup> Likewise, when M<sub>1</sub>dG was placed opposite a two-base bulge, conversion to OpdG was not observed.<sup>54</sup> Riggins et al.<sup>55,56</sup> proposed that the N3-dC imine activates a molecule of water that then adds to the  $\gamma$ -carbon of M<sub>1</sub>dG and catalyzes its conversion to OPdG.

Unlike M<sub>1</sub>dG, the cyclic ring of  $\gamma$ -OH-PdG adduct **2** is not conjugated with the purine ring of dG. Consequently, for  $\gamma$ -OH-PdG, the activation energy barrier with respect to interconversion between cyclic adduct **2** and the aldehyde **3** and hydrated aldehyde **3a** adducts is anticipated

to be lower. The present results suggest that this is in fact the case. When  $\gamma$ -OH-PdG adduct **2** was mispaired with T, an equilibrium mixture of cyclic adduct **2** and the aldehyde **3** and hydrated aldehyde **3a** adducts was observed (Figure 3), suggesting that the presence of dC in the complementary strand was no longer required to facilitate ring-opening.

When T was placed opposite adduct **2**, partial ring-opening was observed at equilibrium, suggesting that opposite T, adduct **2** and its ring-opened counterparts **3** and **3a** exhibit similar energetics in duplex DNA. It seems possible that when placed opposite T, the aldehyde **3** and hydrated aldehyde **3a** adducts stabilize G•T wobble pairing. We surmise that  $\gamma$ -OH-PdG adduct **2** re-orient into the *syn* conformation about the glycosyl bond<sup>12</sup> when mispaired opposite T, placing the cyclic ring into the major groove, a position in which it does not clash sterically with the mispaired T. This may account for the observation that when placed opposite T, cyclic adduct **2** and aldehyde **3** and hydrated aldehyde **3a** adducts are in slow exchange on the NMR time scale. It is of interest to note that in the G•T wobble pair,<sup>57–61</sup> the nucleophilic N1-dG imine of aldehyde adduct **3** hydrogen bonds with O<sup>2</sup> of the mispaired T, positioning it to readily attack the carbonyl of aldehyde **3** and re-cyclize to adduct **2**.

When dA was placed opposite adduct **2**, no ring-opening was observed at equilibrium, suggesting that opposite A, the equilibrium in duplex DNA between adduct **2** and its ring-opened counterparts **3** and **3a** strongly favors the cyclic adduct **2**. We surmise that when mispaired with dA, adduct **2** orients into the *syn* conformation about the glycosyl bond, thus placing the cyclic ring into the major groove and allowing the mispaired dA to hydrogen bond with the Hoogsteen face of the modified dG in a G(*syn*)•A(*anti*) pair.<sup>62</sup> In duplex DNA, the G(*anti*)•A(*anti*)<sup>63,64</sup> and G(*anti*)•A(*syn*)<sup>65</sup> mismatches have also been characterized as to structure. However, these conformations of the G•A mismatch utilize the N1-dG imine as a hydrogen bond donor, which is not possible for adduct **2**.

### Formation of DNA-Peptide Complexes

Previous studies showed that  $\gamma$ -OH-PdG formed DNA-peptide crosslinks mediated by aldehyde **3** and the N-terminal amines of peptides.<sup>13,14</sup> These Schiff base intermediates were reduced by incubation with sodium cyanoborohydride. Thus, monitoring the formation of DNA-peptide complexes allows the presence of aldehydic DNA adduct **3** to be probed. When adduct **2** was examined by <sup>13</sup>C HSQC NMR in single stranded oligodeoxynucleotide (Figure 1) the two epimeric forms of the adduct were detected, but no aldehyde was observed. The presence of low levels of the aldehydic intermediate was inferred from the peptide trapping experiments (Figure 6), consistent with the slow epimerization of adduct **2** in single-strand DNA.<sup>13</sup> Similarly, when adduct **2** was placed opposite dA in duplex DNA, the amount of aldehyde **3** remained below the level the level of detection by <sup>13</sup>C NMR (Figure 5). Nevertheless, the presence of low levels of the aldehyde intermediate can be inferred from the result of peptide trapping experiments (Figure 6). These data are consistent with the epimerization of adduct **2**.

### Summary

Site-specific incorporation of  $\gamma$ -<sup>13</sup>C-OH-PdG and  $\gamma$ -OH-<sup>15</sup>N<sup>2</sup>-PdG into duplex DNA enabled the equilibrium chemistry of this 1,N<sup>2</sup>-dG cyclic adduct to be monitored by NMR, *in situ*. Although interstrand crosslinks in the 5'-CpG-3' sequence context were reductively trapped with NaCNBH<sub>4</sub>, indicating the presence of imine crosslink **5**,<sup>11</sup> the NMR studies revealed that the diastereomeric carbinolamine forms of the crosslinks were favored *in situ*, with the imine (Schiff base) and its pyrimidopurinone rearrangement product remaining below the level of detection. Molecular modeling suggested carbinolamine crosslink **4** maintains Watson-Crick hydrogen bonding at both of the tandem C•G base pairs.

## Supplementary Material

Refer to Web version on PubMed Central for supplementary material.

## Acknowledgements

This work was supported by NIH grant ES-05355 (M.P.S., T.M.H., C.J.R., and R.S.L.). Funding for the NMR spectrometers was supplied by Vanderbilt University; by NIH grant RR-05805, and the Vanderbilt Center in Molecular Toxicology, ES-00267. The Vanderbilt-Ingram Cancer Center is supported by NIH grant CA-68485.

## References

1. Chung FL, Zhang L, Ocando JE, Nath RG. *IARC Sci. Publ* 1999;150:45–54. [PubMed: 10626207]
2. Marnett LJ, Huidr HK, Hollstein MC, Levin DE, Esterbauer H, Ames BN. *Mutat. Res* 1985;148:25–34. [PubMed: 3881660]
3. Smith RA, Cohen SM, Lawson TA. *Carcinogenesis* 1990;11:497–498. [PubMed: 2311195]
4. Curren RD, Yang LL, Conklin PM, Grafstrom RC, Harris CC. *Mutat. Res* 1988;209:17–22. [PubMed: 3173398]
5. Kawanishi M, Matsuda T, Nakayama A, Takebe H, Matsui S, Yagi T. *Mutat. Res* 1998;417:65–73. [PubMed: 9733921]
6. Cohen SM, Garland EM, St John M, Okamura T, Smith RA. *Cancer Res* 1992;52:3577–3581. [PubMed: 1617627]
7. Chung FL, Young R, Hecht SS. *Cancer Res* 1984;44:990–995. [PubMed: 6318992]
8. Chung FL, Krzeminski J, Wang M, Chen HJ, Prokopczyk B. *Chem. Res. Toxicol* 1994;7:62–67. [PubMed: 8155826]
9. Nath RG, Ocando JE, Chung FL. *Cancer Res* 1996;56:452–456. [PubMed: 8564951]
10. Kozekov ID, Nechev LV, Moseley MS, Harris CM, Rizzo CJ, Stone MP, Harris TM. *J. Am. Chem. Soc* 2003;125:50–61. [PubMed: 12515506]
11. Kozekov ID, Nechev LV, Sanchez A, Harris CM, Lloyd RS, Harris TM. *Chem. Res. Toxicol* 2001;14:1482–1485. [PubMed: 11712904]
12. Kim HY, Voehler M, Harris TM, Stone MP. *J. Am. Chem. Soc* 2002;124:9324–9325. [PubMed: 12166998]
13. Kurtz AJ, Lloyd RS. *J. Biol. Chem* 2003;278:5970–5976. [PubMed: 12502710]
14. Sanchez A, Minko I, Kurtz AJ, Kanuri M, Moriya M, Lloyd RS. *Chem. Res. Toxicol* 2003;16:1019–1028. [PubMed: 12924930]
15. Nath RG, Chung FL. *Proc. Natl. Acad. Sci. USA* 1994;91:7491–7495. [PubMed: 8052609]
16. Khullar S, Varaprasad CV, Johnson F. *J. Med. Chem* 1999;42:947–950. [PubMed: 10090776]
17. Nechev LV, Harris CM, Harris TM. *Chem. Res. Toxicol* 2000;13:421–429. [PubMed: 10813660]
18. de los Santos C, Zaliznyak T, Johnson F. *J. Biol. Chem* 2001;276:9077–9082. [PubMed: 11054428]
19. VanderVeen LA, Hashim MF, Nechev LV, Harris TM, Harris CM, Marnett LJ. *J. Biol. Chem* 2001;276:9066–9070. [PubMed: 11106660]
20. Yang I-Y, Johnson R, Grollman AP, Moriya M. *Chem. Res. Toxicol* 2002;15:160–164. [PubMed: 11849041]
21. Yang IY, Hossain M, Miller H, Khullar S, Johnson F, Grollman A, Moriya M. *J. Biol. Chem* 2001;276:9071–9076. [PubMed: 11124950]
22. Yang IY, Chan G, Miller H, Huang Y, Torres MC, Johnson F, Moriya M. *Biochemistry* 2002;41:13826–13832. [PubMed: 12427046]
23. Moriya M, Zhang W, Johnson F, Grollman AP. *Proc. Natl. Acad. Sci. USA* 1994;91:11899–11903. [PubMed: 7991554]
24. Burcham PC, Marnett LJ. *J. Biol. Chem* 1994;269:28844–28850. [PubMed: 7961843]
25. Moriya M. *Proc. Natl. Acad. Sci. USA* 1993;90:1122–1126. [PubMed: 8430083]
26. Kanuri M, Minko IG, Nechev LV, Harris TM, Harris CM, Lloyd RS. *J. Biol. Chem* 2002;277:18257–18265. [PubMed: 11889127]

27. Liu Y-S, Zhao C, Bergbreiter DE, Romo D. *J. Org. Chem* 1998;63:3471–3473.
28. Hunter R, Richards P. *Org. Biomol. Chem* 2003;1:2348–2356. [PubMed: 12945708]
29. Borer, PN. *Handbook of Biochemistry and Molecular Biology*. Cleveland, OH: CRC Press; 1975.
30. Piotto M, Saudek V, Sklenar V. *J. Biomol. NMR* 1992;2:661–665. [PubMed: 1490109]
31. Mori S, Abeygunawardana C, Johnson M, vanZul PCM. *J. Magn. Reson* 1995;108:94–98.
32. Talluri S, Wagner G. *J. Magn. Reson* 1996;112:200–205.
33. Markley JL, Bax A, Arata Y, Hilbers CW, Kaptein R, Sykes BD, Wright PE, Wuthrich K. *J. Mol. Biol* 1998;280:933–952. [PubMed: 9671561]
34. Wishart DS, Bigam CG, Yao J, Abildgaard F, Dyson HJ, Oldfield E, Markley JL, Sykes BD. *J. Biomol. NMR* 1995;6:135–140. [PubMed: 8589602]
35. International Union of Pure and Applied Chemistry. *Pure Appl. Chem* 1998;70:117–142.
36. Delaglio F, Grzesiek S, Vuister GW, Zhu G, Pfeifer J, Bax A. *J. Biomol. NMR* 1995;6:277–293. [PubMed: 8520220]
37. Case, DA., et al. *AMBER, 7.0*. San Francisco, CA: University of California; 2002.
38. Arnott S, Hukins DWL. *Biochem. Biophys. Res. Comm* 1972;47:1504–1509. [PubMed: 5040245]
39. Frisch, MJ.; Trucks, GW., et al. *GAUSSIAN98*. Pittsburgh, PA: Gaussian, Inc.; 1998.
40. Tsui V, Case DA. *Biopolymers* 2000;56:275–291. [PubMed: 11754341]
41. Bashford D, Case DA. *Annu. Rev. Phys. Chem* 2000;51:129–152. [PubMed: 11031278]
42. Wang H, Kozekov ID, Harris TM, Rizzo CJ. *J. Am. Chem. Soc* 2003;125:5687–5700. [PubMed: 12733907]
43. DeCorte BL, Tsarouhtsis D, Kuchimanchi S, Cooper MD, Horton P, Harris CM, Harris TM. *Chem. Res. Toxicol* 1996;9:630–637. [PubMed: 8728509]
44. Harris CM, Zhou L, Strand EA, Harris TM. *J. Am. Chem. Soc* 1991;113:4328–4329.
45. Ramu K, Fraiser LH, Mamiya B, Ahmed T, Kehrer JP. *Chem. Res. Toxicol* 1995;8:515–524. [PubMed: 7548731]
46. Basu AK, O'Hara SM, Valladier P, Stone K, Mols O, Marnett LJ. *Chem. Res. Toxicol* 1988;1:53–59. [PubMed: 2979712]
47. Marnett LJ, Basu AK, O'Hara SM, Weller PE, Rahman AFMM, Oliver JP. *J. Am. Chem. Soc* 1986;108:1348–1350.
48. Seto H, Seto T, Takesue T, Ikemura T. *Chem. Pharm. Bull* 1986;34:5079–5085. [PubMed: 2436822]
49. Seto H, Okuda T, Takesue T, Ikemura T. *Bull. Chem. Soc. Jpn* 1983;56:1799–1802.
50. Reddy GR, Marnett LJ. *Chem. Res. Toxicol* 1996;9:12–15. [PubMed: 8924580]
51. Dedon PC, Plastaras JP, Rouzer CA, Marnett LJ. *Proc. Natl. Acad. Sci. USA* 1998;95:11113–11116. [PubMed: 9736698]
52. Mao H, Schnetz-Boutaud NC, Weisenseel JP, Marnett LJ, Stone MP. *Proc. Natl. Acad. Sci. USA* 1999;96:6615–6620. [PubMed: 10359760]
53. Mao H, Reddy GR, Marnett LJ, Stone MP. *Biochemistry* 1999;38:13491–13501. [PubMed: 10521256]
54. Schnetz-Boutaud NC, Saleh S, Marnett LJ, Stone MP. *Biochemistry* 2001;40:15638–15649. [PubMed: 11747439]
55. Riggins JN, Daniels JS, Rouzer CA, Marnett LJ. *J. Am. Chem. Soc* 2004;126:8237–8243. [PubMed: 15225065]
56. Riggins JN, Pratt DA, Voehler M, Daniels JS, Marnett LJ. *J. Am. Chem. Soc* 2004;126:10571–10581. [PubMed: 15327313]
57. Kneale G, Brown T, Kennard O, Rabinovich D. *J. Mol. Biol* 1985;186:805–814. [PubMed: 4093986]
58. Brown T, Kennard O, Kneale G, Rabinovich D. *Nature* 1985;315:604–606. [PubMed: 4010774]
59. Kennard O. *J. Biomol. Struct. Dyn* 1985;3:205–226. [PubMed: 3917021]
60. Hare D, Shapiro L, Patel DJ. *Biochemistry* 1986;25:7445–7456. [PubMed: 3801424]
61. Kalnik MW, Kouchakdjian M, Li BFL, Swann PF, Patel DJ. *Biochemistry* 1988;27:108–115. [PubMed: 3349021]
62. Gao X, Patel DJ. *J. Am. Chem. Soc* 1988;110:5178–5182.

63. Kan LS, Chandrasegaran S, Pulford SM, Miller PS. Proc. Natl. Acad. Sci. USA 1983;80:4263–4265. [PubMed: 6576336]
64. Patel DJ, Kozlowski SA, Ikuta S, Itakura K. Biochemistry 1984;23:3207–3217. [PubMed: 6466638]
65. Hunter WN, Brown T, Kennard O. J. Biomol. Struct. Dyn 1986;4:173–191. [PubMed: 3271438]

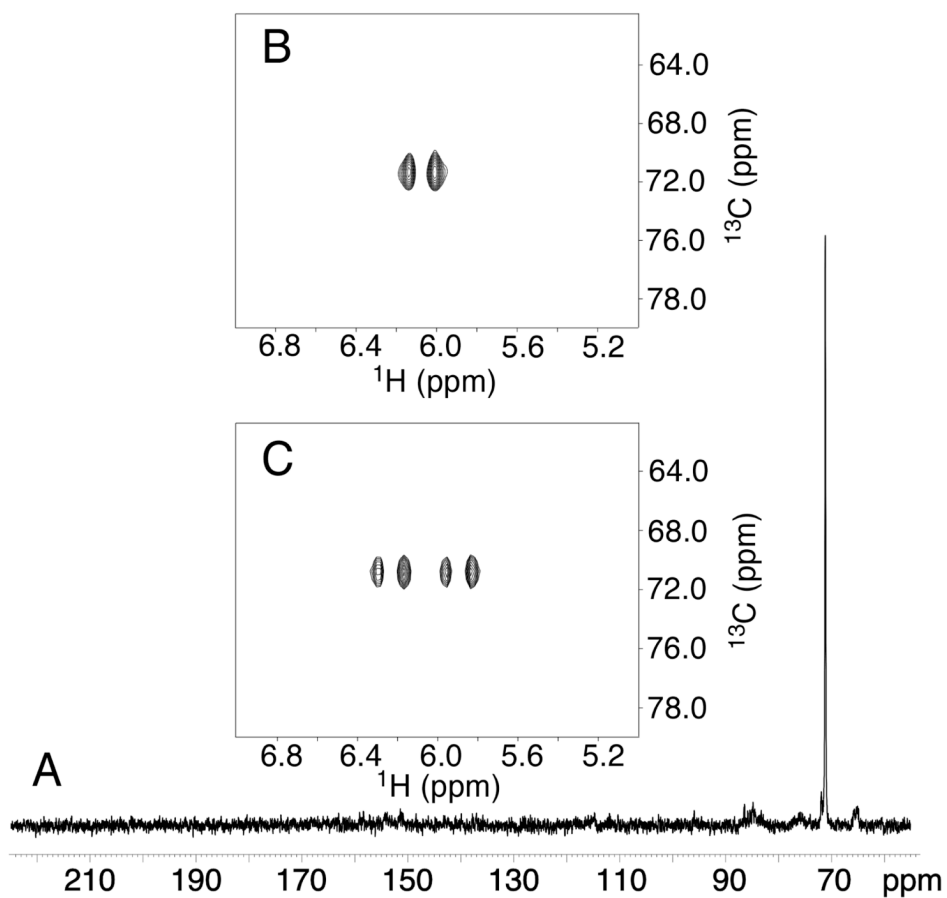


**Figure 1.** **A.**  $^{13}\text{C}$  spectrum of single-stranded oligodeoxynucleotide **18**, 5'-d(GCTAGCXAGTCC)-3'; X =  $\gamma$ - $^{13}\text{C}$ -OH PdG adduct **2**. **B.**  $^1\text{H}$ -decoupled  $^{13}\text{C}$  HSQC spectrum. **C.**  $^1\text{H}$ -coupled  $^{13}\text{C}$  HSQC spectrum. The spectra show the presence of two epimers of the  $\gamma$ - $^{13}\text{C}$ -OH PdG adduct **2**.



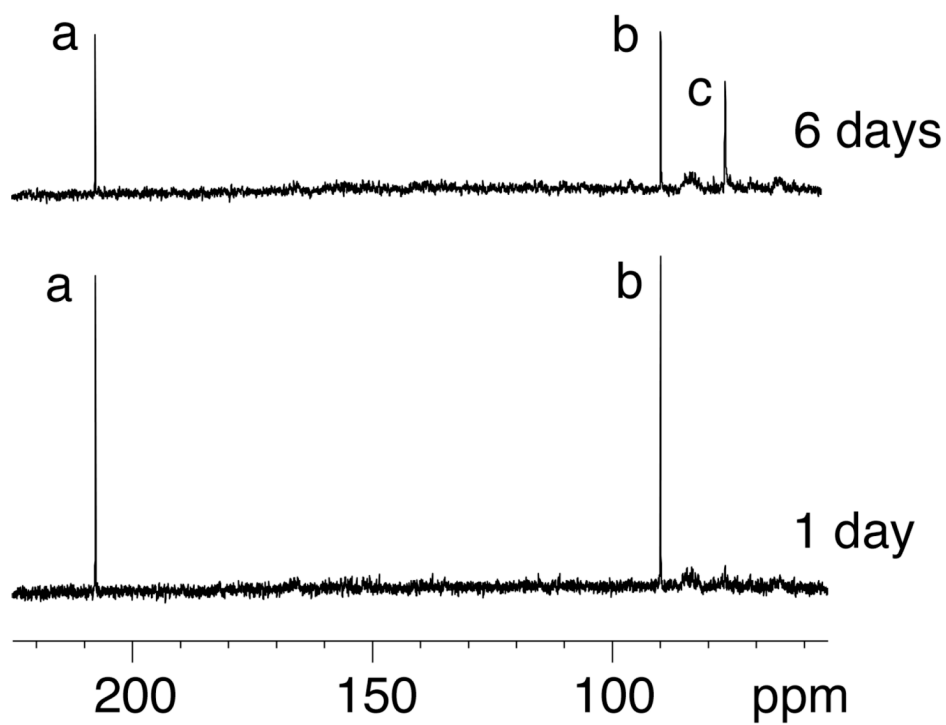


**Figure 2.**  $^{13}\text{C}$  spectrum of oligodeoxynucleotide **18** annealed with its complement to yield the duplex 5'-d(GCTAGCXAGTCC)-3'•5'-d(GGACTCGCTAGC)-3', X= $\gamma$ - $^{13}\text{C}$ -OH PdG, adduct **2**. The bottom spectrum was collected in the first day after annealing the duplex. The top spectrum was collected after 6 days at 37 °C. Assignments of resonances: a, aldehyde **3**; b, hydrated-aldehyde **3a**; c, carbinolamines **4**.

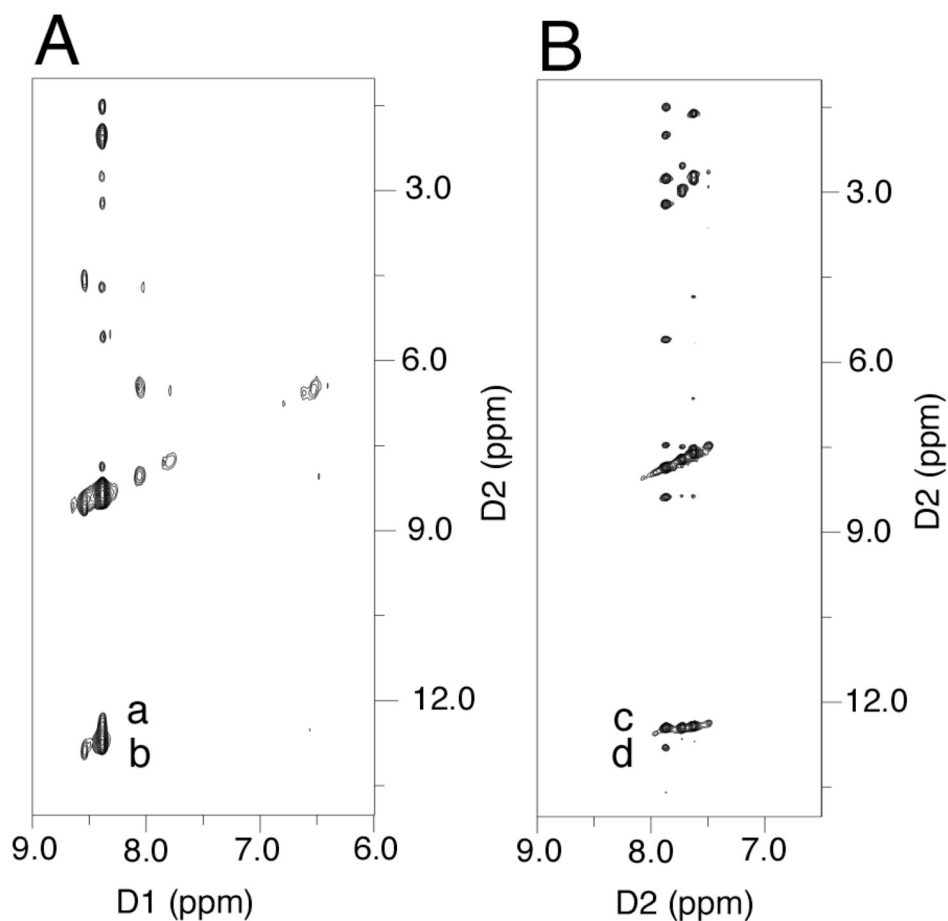


**Figure 3.**

$^{15}\text{N}$ -NOESY HSQC spectra indicate that both base pairs in the 5'-CpG-3'  $\gamma$ -OH-PdG induced interstrand crosslink remain intact. **A.**  $^{15}\text{N}$ -NOESY HSQC spectrum for  $^{15}\text{N}^2$ -dG labeled oligodeoxynucleotide **22** annealed with its complement to yield the duplex 5'-d(G<sup>1</sup>C<sup>2</sup>T<sup>3</sup>A<sup>4</sup>G<sup>5</sup>C<sup>6</sup>X<sup>7</sup>A<sup>8</sup>G<sup>9</sup>T<sup>10</sup>C<sup>11</sup>C<sup>12</sup>)-3'•5'-d(G<sup>13</sup>G<sup>14</sup>A<sup>15</sup>C<sup>16</sup>T<sup>17</sup>C<sup>18</sup>Y<sup>19</sup>C<sup>20</sup>T<sup>21</sup>A<sup>22</sup>G<sup>23</sup>C<sup>24</sup>)-3', X<sup>7</sup>= $\gamma$ -OH PdG, adduct **2**; Y<sup>19</sup>= $^{15}\text{N}^2$ -dG.<sup>12</sup> Crosspeaks a, Y<sup>19</sup>  $^{15}\text{N}^2\text{H}$ →X<sup>7</sup> N1H (weak); b, Y<sup>19</sup>  $^{15}\text{N}^2\text{H}$ →Y<sup>19</sup> N1H (strong). **B.**  $^{15}\text{N}$ -HSQC NOESY spectrum for  $\gamma$ -OH- $^{15}\text{N}^2$ -PdG labeled oligodeoxynucleotide **20** annealed with its complement to yield the duplex 5'-d(G<sup>1</sup>C<sup>2</sup>T<sup>3</sup>A<sup>4</sup>G<sup>5</sup>C<sup>6</sup>X<sup>7</sup>A<sup>8</sup>G<sup>9</sup>T<sup>10</sup>C<sup>11</sup>C<sup>12</sup>)-3'•5'-d(G<sup>13</sup>G<sup>14</sup>A<sup>15</sup>C<sup>16</sup>T<sup>17</sup>C<sup>18</sup>G<sup>19</sup>C<sup>20</sup>T<sup>21</sup>A<sup>22</sup>G<sup>23</sup>C<sup>24</sup>)-3', X<sup>7</sup>= $\gamma$ -OH- $^{15}\text{N}^2$ -PdG, adduct **2**. Crosspeaks c, X<sup>7</sup>  $\gamma$ -OH-PdG  $^{15}\text{N}^2\text{H}$ →X<sup>7</sup>  $\gamma$ -OH-PdG N1H (strong); d, X<sup>7</sup>  $\gamma$ -OH-PdG  $^{15}\text{N}^2\text{H}$ →G<sup>19</sup> N1H (weak).

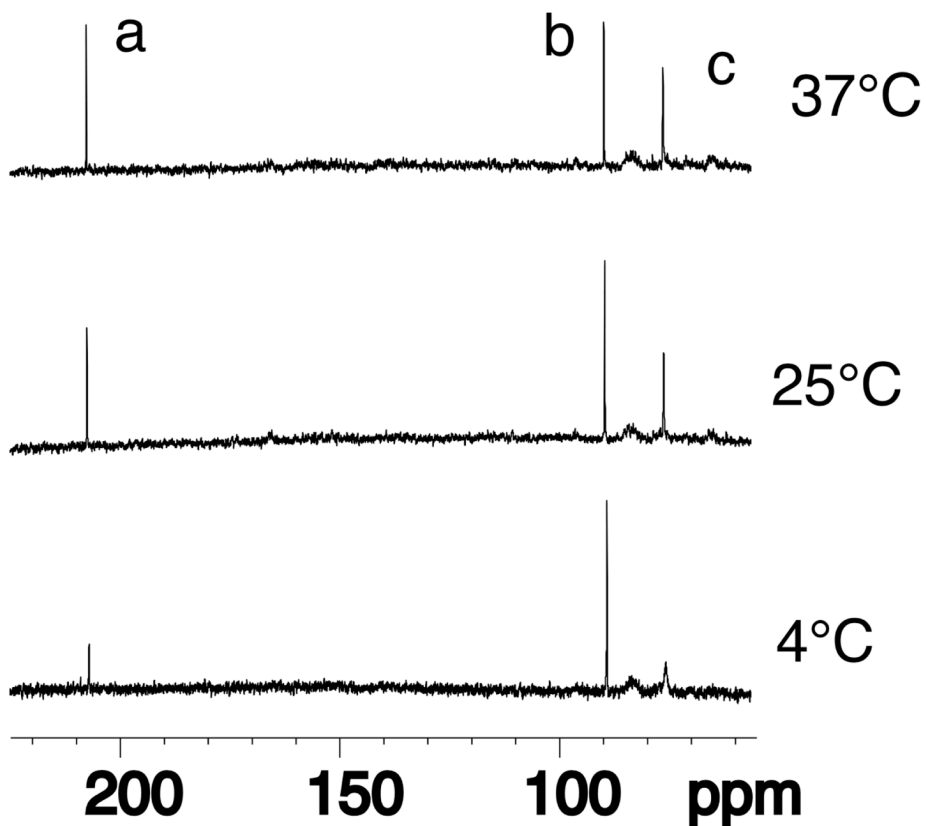


**Figure 4.**  $^{13}\text{C}$  spectrum of oligodeoxynucleotide **18** annealed with its complement to yield the duplex 5'-d(GCTAGCXAGTCC)-3'•5'-d(GGACTCGCTAGC)-3', X= $\gamma$ - $^{13}\text{C}$ -OH PdG, adduct **2**, collected as a function of temperature. The bottom spectrum was collected at 4 °C, the middle spectrum at 25 °C, and the top spectrum at 37 °C. Assignments of resonances: a, aldehyde **3**; b, hydrated-aldehyde **3a**; c, carbinolamines **4**.

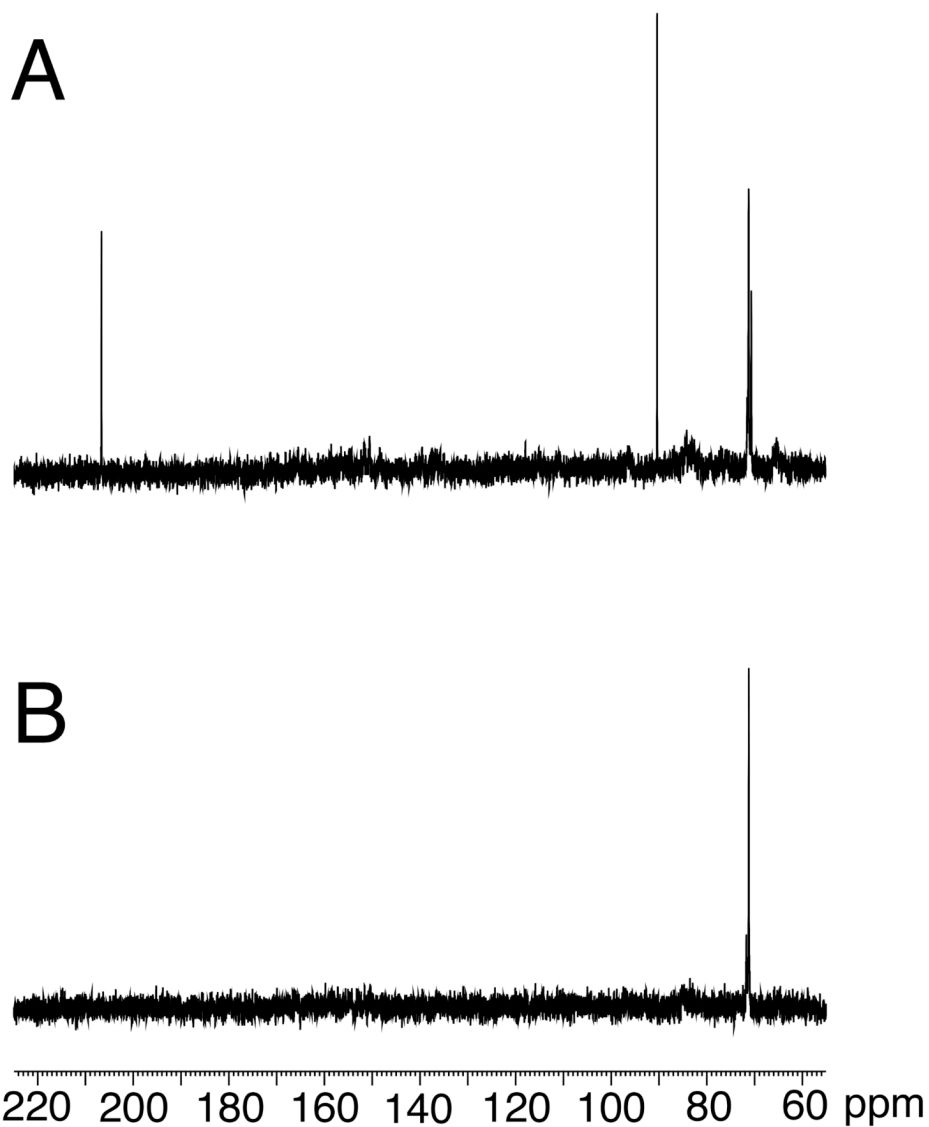


**Figure 5.**

**A.**  $^{13}\text{C}$  spectrum of oligodeoxynucleotide **18** annealed with its mismatched complement to yield the X•T duplex 5'-d(GCTAGCXAGTCC)-3'•5'-d(GGACTTGCTAGC)-3' duplex, X= $\gamma$ - $^{13}\text{C}$ -OH PdG, adduct **2**. **B.**  $^{13}\text{C}$  spectrum of oligodeoxynucleotide **18** annealed with its mismatched complement to yield the X•A duplex 5'-d(GCTAGCXAGTCC)-3'•5'-d(GGACTAGCTAGC)-3' duplex, X= $\gamma$ - $^{13}\text{C}$ -OH PdG, adduct **2**.

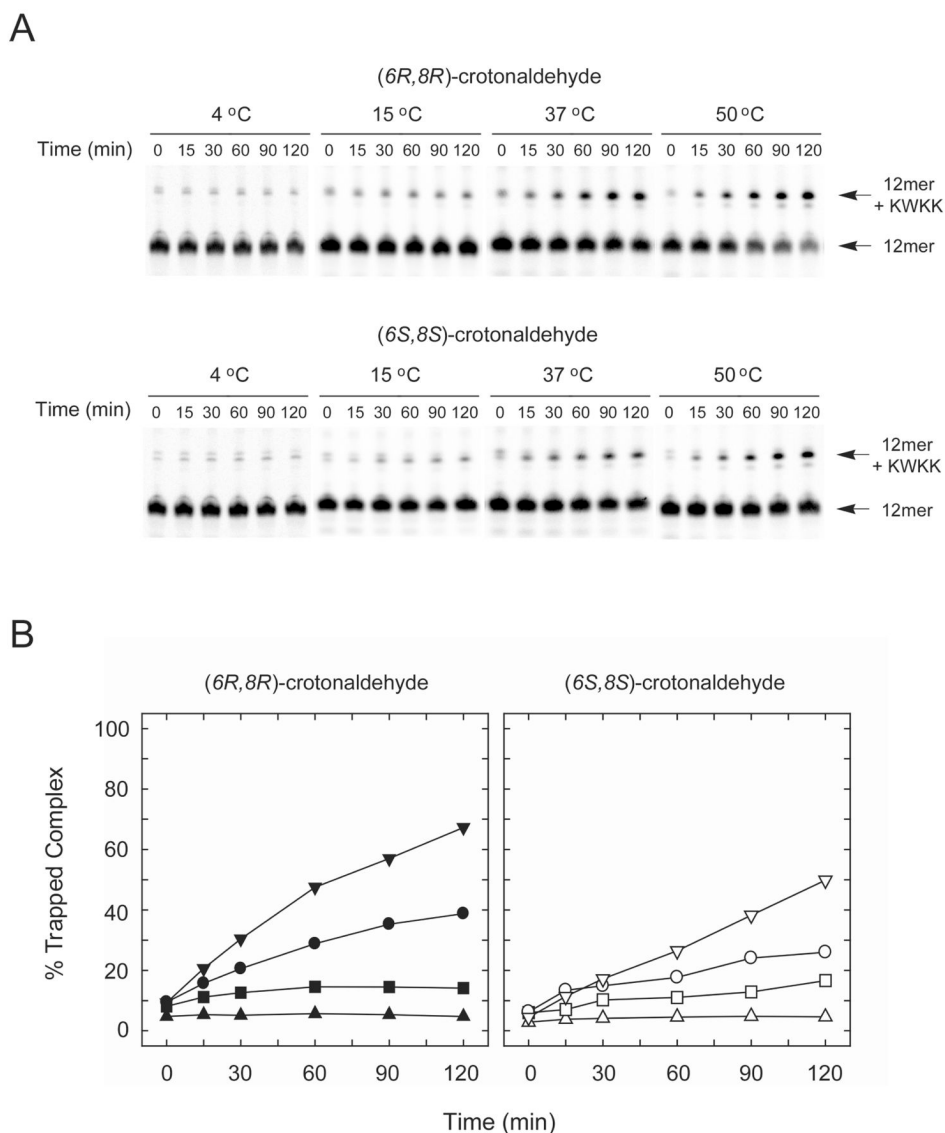


**Figure 6.** Accumulation of the trapped DNA-peptide complexes formed by  $\gamma$ -OH-PdG-modified oligodeoxynucleotides in single-stranded (ss  $\gamma$ -OH-PdG) and double-stranded DNAs containing either  $\gamma$ -OH-PdG•A or  $\gamma$ -OH-PdG•T mismatch. **A.** PAGE analyses of the trapping reactions. The positions of the 58-mer oligodeoxynucleotides and the 58-mer oligodeoxynucleotides cross-linked with the KWKK tetrapeptide are indicated. **B.** Kinetic analyses of the accumulation of the trapped complexes.

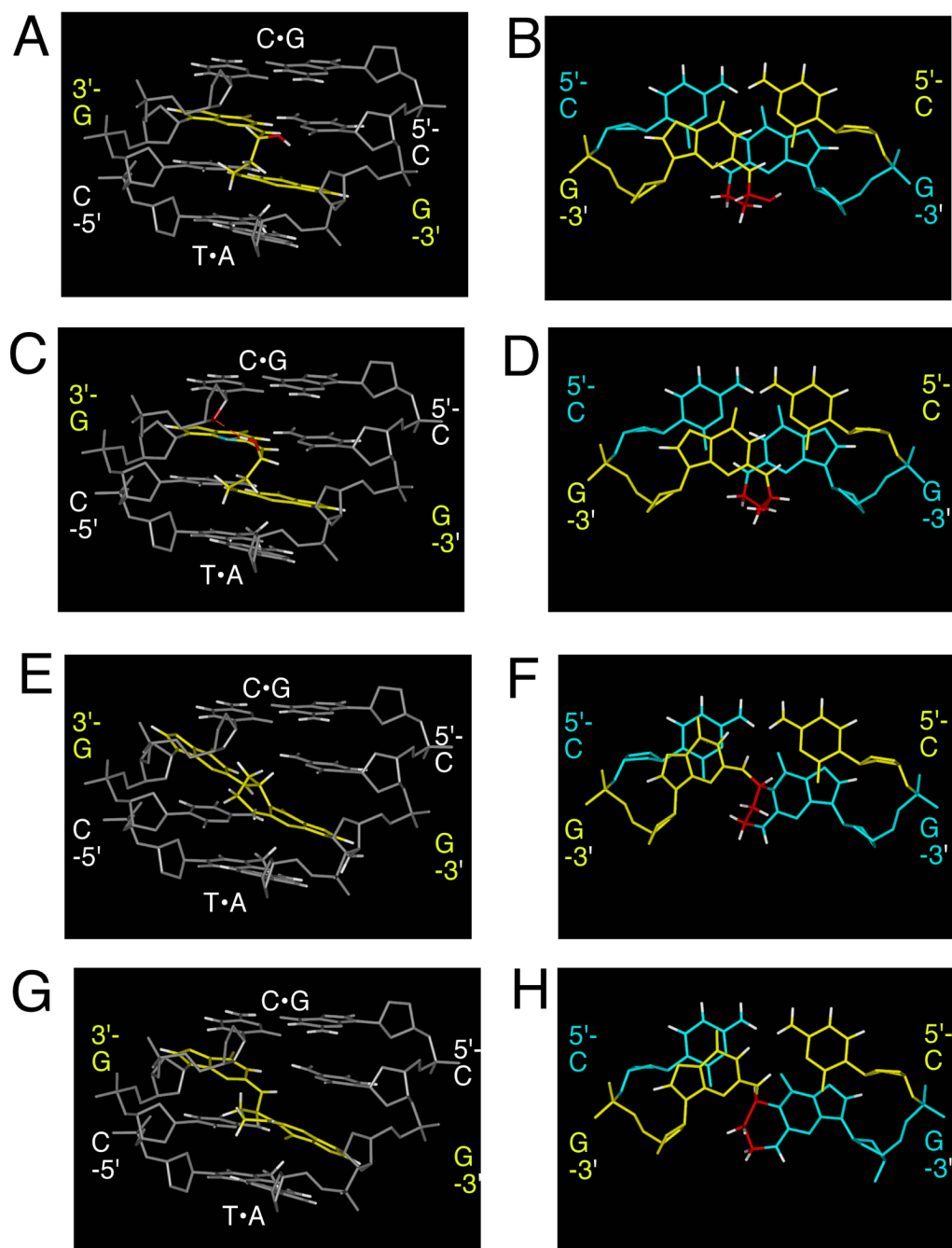
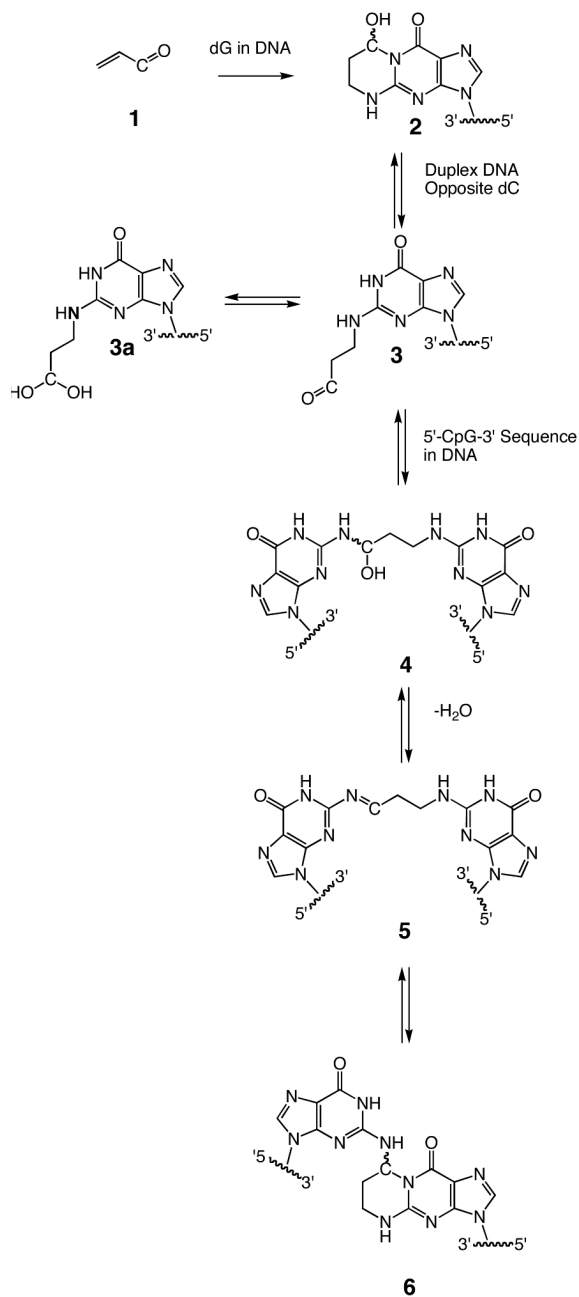


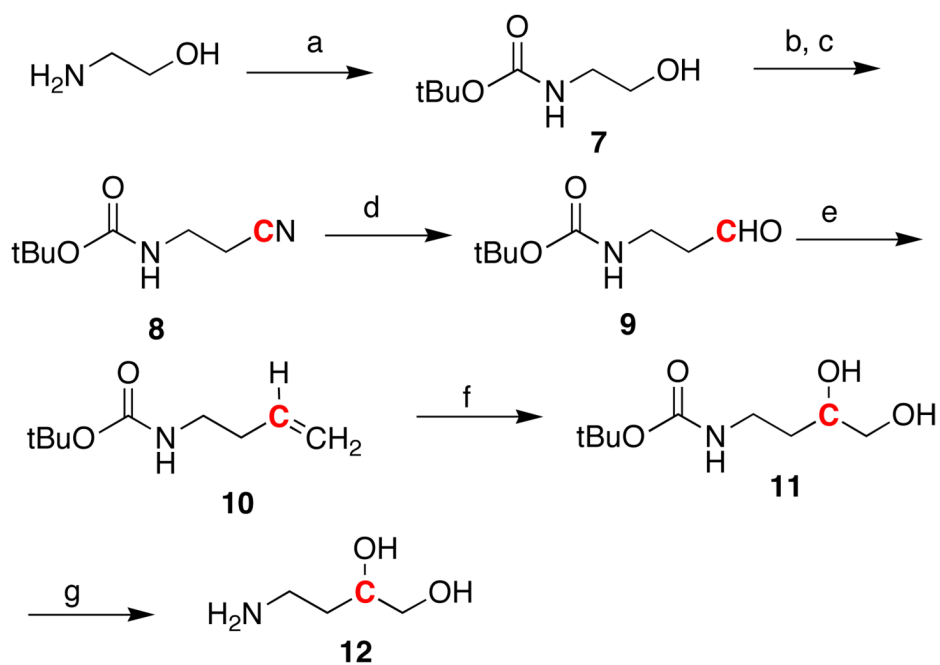
**Figure 7.** Molecular modeling studies acrolein-induced interstrand crosslinking in the 5'-CpG-3' DNA sequence context. In all instances the 5'-flanking base pair to the 5'-CpG-3' DNA sequence context is a C•G base pair; the 3' flanking base pair is an T•A base pair. **A.** *R*-diastereomer of carbinolamine crosslink **4**, viewed from the minor groove. **B.** *R*-diastereomer of carbinolamine crosslink **4**, base stacking interactions. **C.** *S*-diastereomer of carbinolamine crosslink **4**, viewed from the minor groove. **D.** *S*-diastereomer of carbinolamine crosslink **4**, base stacking interactions. **E.** *R*-diastereomer of pyrimidopurinone crosslink **6**, viewed from the minor groove. **F.** *R*-diastereomer of pyrimidopurinone crosslink **6**, base stacking interactions. **G.** *S*-diastereomer of pyrimidopurinone crosslink **6**, viewed from the minor groove. **H.** *S*-diastereomer of pyrimidopurinone crosslink **6**, base stacking interactions.

diastereomer of pyrimidopurinone crosslink **6**, viewed from the minor groove. **H.** *S*-diastereomer of pyrimidopurinone crosslink **6**, base stacking interactions.

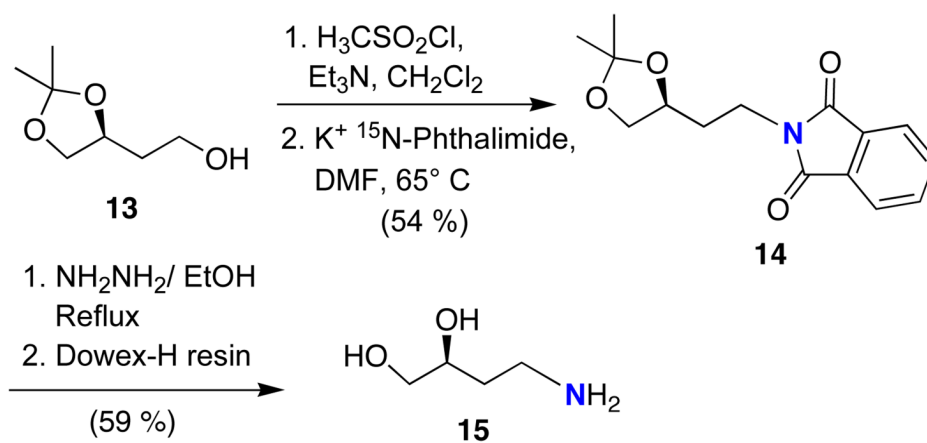


**Scheme 1.**  
Equilibrium Chemistry of the  $\gamma$ -OH-PdG Adduct in the 5'-CpG-3' Sequence in Duplex DNA.

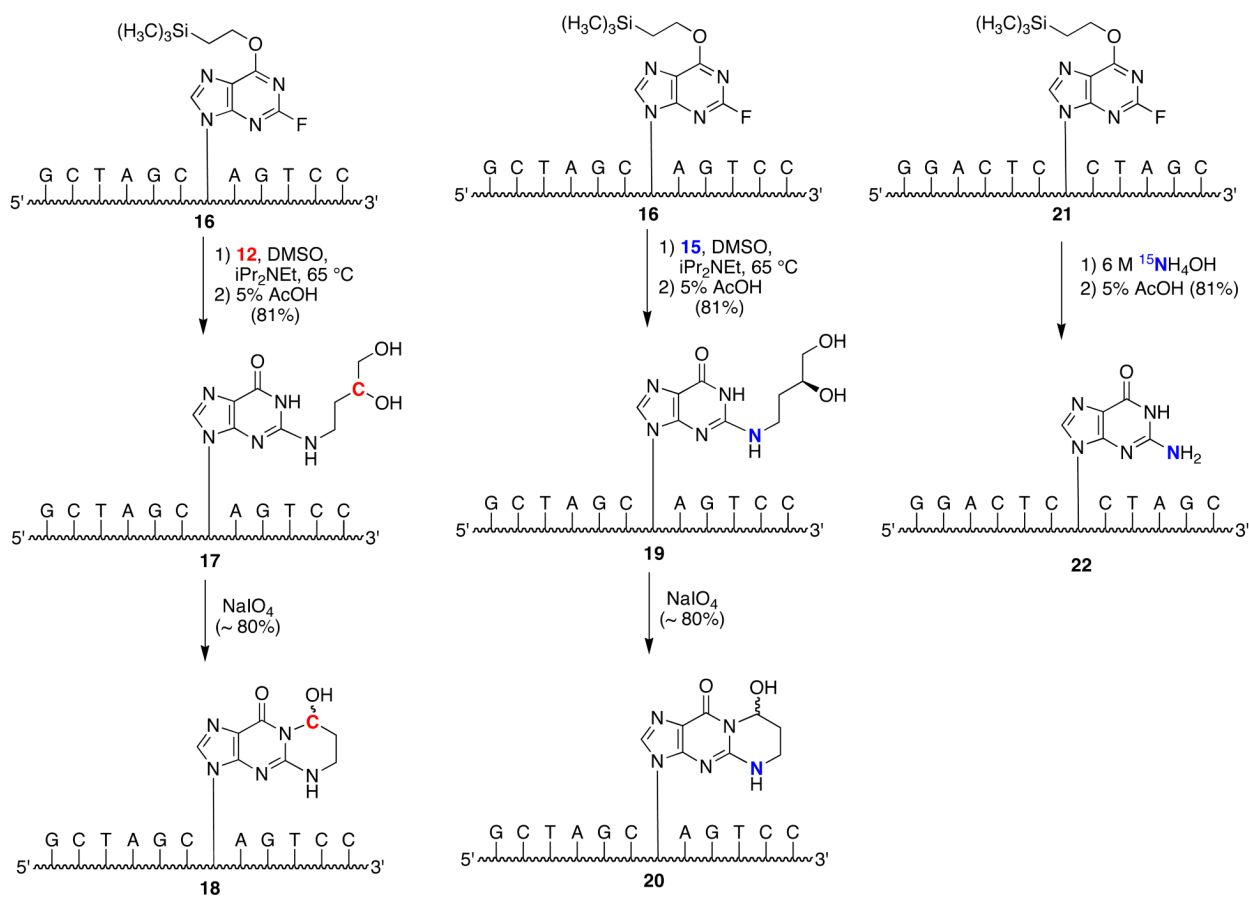


**Scheme 2.**

Synthesis of the  $^{13}\text{C}$  aminodiol, 4-Amino-2- $^{13}\text{C}$ -butane-1,2-diol (**12**). a)  $(t\text{BuCO})_2\text{O}$ , NaOH, b) MsCl,  $\text{Et}_3\text{N}$ , 70% c)  $\text{K}^{13}\text{CN}$ , DMSO,  $40^\circ\text{C}$ , 70% for two steps d) DiBAI-H,  $\text{CH}_2\text{Cl}_2$ ,  $-78^\circ\text{C}$ ; acetone,  $-78^\circ\text{C} \rightarrow \text{RT}$ ; then saturated aqueous  $\text{NH}_4\text{Cl}$ , 30% e)  $\text{Ph}_3\text{P}^+\text{CH}_3\text{Br}^-$ ,  $t\text{-BuO-K}^+$ , THF, 65% f)  $\text{OsO}_4$ , NMO, THF,  $\text{H}_2\text{O}$ , 69% g) Amberlyst-15  $\text{H}^+$ , 91%



**Scheme 3.**  
Synthesis of the  $^{15}\text{N}$  aminodiol,  $4\text{-}^{15}\text{N}$ -amino-2-butane-1,2-diol (**15**).



**Scheme 4.**  
Synthesis of Oligodeoxynucleotides Containing Site-Specific <sup>15</sup>N, <sup>13</sup>C Isotopes.